Copyright Warning & Restrictions

The copyright law of the United States (Title 17, United States Code) governs the making of photocopies or other reproductions of copyrighted material.

Under certain conditions specified in the law, libraries and archives are authorized to furnish a photocopy or other reproduction. One of these specified conditions is that the photocopy or reproduction is not to be "used for any purpose other than private study, scholarship, or research." If a, user makes a request for, or later uses, a photocopy or reproduction for purposes in excess of "fair use" that user may be liable for copyright infringement,

This institution reserves the right to refuse to accept a copying order if, in its judgment, fulfillment of the order would involve violation of copyright law.

Please Note: The author retains the copyright while the New Jersey Institute of Technology reserves the right to distribute this thesis or dissertation

Printing note: If you do not wish to print this page, then select "Pages from: first page # to: last page #" on the print dialog screen

HEAT TRANSFER CHARACTERISTICS

OF

NON-NEWTONIAN SUSPENSIONS

A THESIS
SUBMITTED TO THE FACULTY OF
THE DEPARTMENT OF CHEMICAL ENGINEERING
OF
NEWARK COLLEGE OF ENGINEERING

by

HAROLD BINDER

B. Ch. E.

and

PAUL POLLARA

B. Ch. E.

IN PARTIAL FULFILLMENT OF THE REQUIREMENTS FOR THE
DEGREE OF MASTER OF SCIENCE IN CHEMICAL ENGINEERING.

NEWARK, NEW JERSEY

May - 1954

APPROVAL OF THESIS

FOR

DEPARTMENT OF CHEMICAL ENGINEERING

NEWARK COLLEGE OF ENGINEERING

BY

FACULTY COMMITTEE

APPROVED: Dr. Jerome J. Salamone (Advisor)

NEWARK, NEW JERSEY

MAY - 1954

TABLE of CONTENTS

ACKNOWLEDGEMENT

The authors express their sincere appreciation to Dr. Jerome J. Salamone for his assistance, confidence, interest and guidance in carrying this project to a successful conclusion.

The authors gratefully acknowledge the sincere efforts of Mr. William Furmadge who assisted in the construction of the elaborate apparatus required for the work herein described.

The authors wish to acknowledge their collaborators in this work, Mr. Robert G. Quinn and Mr. Irving Bauman, who shared in this work of constructing the apparatus and collecting the necessary data.

LIST OF FIGURES

ABSTRACT

The following equation was developed by Dr. J. J. Salamone for calculating the film coefficient of heat transfer to non-Newtonian suspensions in turbulent flow (Re 50,000 - 200,000) inside of pipes:

$$\frac{hD}{K_f} = 0.131 \left(\frac{DV_b\rho_b}{u_b}\right)^{0.62} \left(\frac{D}{D_s}\right)^{0.05} \left(\frac{C_s}{C_f}\right)^{0.35} \left(\frac{C_{fu_b}}{K_f}\right)^{0.72} \left(\frac{K_s}{K_f}\right)^{0.05}$$

This equation was investigated to determine its validity over the lower turbulent regions of the Reynolds number (10,000 - 70,000), and to test the exponents of the various components.

Equipment was constructed similar to that used in the original investigation with added improvements from which it was hoped to gain more accuracy.

The results of the correlated data showed the following equation to be valid:

$$\frac{hD}{K_f} = 0.346 \left(\frac{DV_b\rho_b}{u_b}\right)^{0.7} \left(\frac{D_s}{D}\right)^{0.152} \left(\frac{C}{C_s}\right)^{0.35} \left(\frac{C_{fu_b}}{K_f}\right)^{0.72} \left(\frac{K_s}{K_f}\right)^{0.08}$$

The original investigation also showed that the effective thermal conductivity varied with velocity and reached some limiting value at full turbulence, which was corroborated by this investigation.

The calculated data further substantiated that certain properties of the slurry utilized in this equation such as bulk velocity, bulk density, and bulk viscosity, heretofore not used in equations, could be used for designing heat transfer equipment for non-Newtonian suspensions.

INTRODUCTION

The object of this research was to check an equation developed by Dr. J. J. Salamone for predicting the film coefficient of heat transfer for non-Newtonian suspensions in turbulent flow. His investigation was prompted by the lack of such an equation and by the hypothesis gained from fragmentary data that suspensions of finely divided solid particles of high thermal conductivities in a liquid medium would improve the heat transfer properties of the liquid.

The equation referred to above was developed from a majority of data collected in the 50,000 - 200,000 Reynolds number range. In the present investigation it was decided to collect data in the 10,000 - 70,000 Reynolds number range and from that data re-calculate several of the exponents involved in the original equation and thereby obtain a check of the equation over most of the turbulent flow region.

The equation referenced above was one developed by dimensional analysis. The second approach to the problem was investigated under the assumption that the present equations for liquids could be applied to suspensions, provided that the properties involved could be evaluated for the suspension. It was found that all the properties except the bulk viscosity and the effective thermal conductivity of the suspension could be evaluated. The

effective thermal conductivity and the bulk viscosity were evaluated by calibrating the experimental apparatus with water. The investigation showed that above a Reynolds number of 37,500 the effective thermal conductivity for each suspension reached some limiting value that was greater than that of the dispersion medium. From the limiting value a linear equation was written. The effective thermal conductivities calculated were found to be applicable to the Dittus Boelter equation.

This thesis of Binder and Pollara is one of two which ran concurrently with that of Bauman and Quinn.

It was the purpose of this half of the work to determine the exponent of the expression K_s/K_f, calculate effective thermal conductivities and compare their trend in a plot of K_e versus Reynolds number to the trend found by Salamone, and to compare his correlation to the new correlation using the new exponents.

Quinn and Bauman investigated the exponent of the Reynolds number and of the particle size expression (D/D_s).

The data and figures of both parts of this work are shown in each thesis for the convenience of the reader.

THEORY

The newest formulak for predicting the coefficient of heat transfer (h) to non-Newtonian solutions of the pseudoplastic type was developed theoretically by J. J. Salamone through the use of dimensional analysis. He concluded that the film coefficient of heat transfer should be a function of:

pipe diameter - D

weight fraction of solid - X

thermal conductivity of the dispersion medium - K_f

average particle diameter - D_s

particle shape

specific heat of solid - C_s

specific heat of dispersion medium - C_f

density of solid - p_s

density of dispersion medium - p_f

apparent bulk viscosity of the suspension - u_b

velocity, based on bulk density - V_b

Assuming spherical particles and incorporating density of the solid, of the dispersion medium, and weight fraction of solid into a bulk density of the suspension p_b. Then by dimensional analysis the following equation was derived:

$$\frac{hD}{u_b C_f} = Z \left(\frac{DV_b p_b}{u_b}\right)^b \left(\frac{K_f}{u_b C_f}\right)^g \left(\frac{K_s}{u_b C_f}\right)^n \left(\frac{D_s}{D}\right)^r \left(\frac{C_s}{C_f}\right)^j \quad \text{Eq. (1)}$$

The constants in the above equation were then determined from experimental data and yielded the following form of the equation:

$$\frac{hD}{u_b C_f} = 0.131 \left(\frac{DV_b P_b}{u_b}\right)^{0.62} \left(\frac{K_f}{u_b C_f}\right)^{0.23} \left(\frac{K_s}{u_b C_f}\right)^{0.05} \left(\frac{D}{D_s}\right)^{0.05} \left(\frac{C_s}{C_f}\right)^{0.35} \quad \text{Eq. (2)}$$

multiply both sides by $u_b C_f$ and rearranging to give

$$\frac{hD}{K_f} = 0.131 \left(\frac{DV_b P_b}{u_b}\right)^{0.62} \left(\frac{D}{D_s}\right)^{0.05} \left(\frac{C_s}{C_f}\right)^{0.35} \left(\frac{C_f u_b}{K_f}\right)^{0.72} \left(\frac{K_s}{K_f}\right)^{0.05} \quad \text{Eq. (3)}$$

From inspection of the above equation it can be seen that variations in u, greatly effect the size of the heat transfer coefficient h. The value of u depends upon the type of fluid used.

Fluids have been found to fall into two general categories, Newtonian and non-Newtonian. A plot of shearing stress versus time rate of shearing strain gives a straight line through the origin for Newtonian fluids. The viscosity is equal to the slope of this line and is constant for any one temperature and pressure.

For a non-Newtonian fluid the ratio of stress to strain is a function of the time rate of shearing strain and therefore the apparent viscosity depends upon rate of flow.

The flow of suspensions has been shown by previous investigators to be non-Newtonian, -- and that many are

of the pseudoplastic type -- where the apparent viscosity decreases with increasing velocity. Data for the stress strain curve for determining the apparent viscosity may best be obtained from a pipe line viscometer.

These viscosities are based on the Fanning friction equation:

$$\frac{-\Delta P}{p} = f \frac{LV^2}{D2g_c} \qquad \text{Eq. (4)}$$

In order to use the pressure drop data from the viscometer it is first calibrated with a Newtonian fluid whose density and viscosity is known and a plot of friction factor (f) versus Reynolds number (Re) made from this experimental data. Then by calculating a friction factor using the bulk density and pressure drop of the slurry a corresponding Reynolds number can be found and the bulk viscosity calculated.

From the above, it logically follows that the pipe line viscosity for slurries determined under the same conditions that the heat transfer data was obtained is the one that should be used for correlating that data.

This is especially true in the case of pseudoplastics where the viscosity decreases with increase velocity until it reaches some limiting value at complete turbulence where its viscosity is still greater than that of the dispersion medium.

LITERATURE SEARCH

A search was made into the available literature to determine the extent of the work performed by other investigators, to obtain sufficient background for designing the apparatus required, and to organize the experimental work to obtain sufficient data for use in arriving at valid conclusions.

The first engineering investigations on the flow behavior of non-Newtonian fluids in conduits appeared in the work of Wilhelm, Wroughton, and Loeffel (18) at Princeton University and Caldwell and Babbitt (3) at the University of Illinois. The purpose of this work deals primarily with the determination of a procedure for correlating pressure drops for various suspensions. Heretofore, only qualitative information based on minor experimental data had been available. Babbitt and Caldwell used sewage sludge and aqueous suspensions of clay, sand and wood pulp, considering sewage sludge and clay slurries as true plastics. The coefficient of rigidity and the yield value of a sludge were found to be independent of the velocity of flow and the pipe dimensions, but dependent upon the concentration of suspended material, size and character of this material, nature of the continuous phase, temperature, slippage and seepage, gas content and agitation. Their data showed that for a given concentra-

tion of suspension, the finer the particle size, the greater the resistance to flow. Agitation was shown to have a definite effect on flow characteristics by a change in particle size and distribution. Density was shown to be unimportant in the laminar or streamline flow region, but of definite effect on the friction factor above the critical velocity which is that velocity below which the friction loss follows the plastic flow equations of Bingham (5) and above which the friction loss is directly proportional to some power of the velocity between 1.7 and 2.0. Their data on suspensions of clay and sewage sludge indicate in the turbulent flow region that the conventional Reynolds number versus friction factor plot, is valid if the viscosity of the dispersion medium is used. The yield value and the rigidity coefficient have no effect on the friction factor in the turbulent region as measured by pressure drop in known sizes and lengths of pipe. This is so, since, in turbulent flow the friction loss is due to impact kinetic energy loss which in turn depends only on the density of the material flowing and its velocity; or, suspended material effects the density but not the viscosity in the turbulent region.

Wilhelm, (17) et al. employed water suspensions of cement rock and Filter-Cel, varying in concentration from 54 to 62% and 21 to 34% solids, respectively, and ran them

simultaneously in a modified Stormer Viscosimeter and in pressure drop sections of known pipe size and length. For cement rock suspensions pronounced deviations from Newtonian properties were found at low rates of shear (fluid velocity in pipe sections, and RPM in viscosimeter), while at high velocities the suspensions behaved similar to a liquid more viscous than water. Filter-Cel slurries more closely resembled a true fluid of greater viscosity than water. For both cases viscosity increased with concentration. The pressure drop data obtained could be correlated on the conventional friction factor plot, if a corrected viscosity was employed. This corrected value, which might bereferred to as the turbulent viscosity as proposed by Binder and Busher (4) was obtained from a plot of Log Z versus the RPM of the viscosimeter by extrapolating the straight line obtained to zero shear, or RPM. Log Z is defined as the viscosity that a true fluid would have for the same friction factor as a non-Newtonian fluid where the friction factor is defined for the viscosimeter as the torque divided by the specific gravity and the square of the RPM, and the Reynolds number as RPM times the specific gravity divided by Z.

Two additional papers have appeared; one on true plastic and the other on pseudoplastic fluids which substantiate the data of Wilhelm and his workers. Binder

and Busher (4) used suspensions of grain in water and prepared data which indicated that, for true plastics, data can be correlated in the turbulent region by an equivalent, or turbulent viscosity which is the viscosity of a true fluid having the same friction factor as the plastic for flow through pipes. The parts of a paper by Winding et al. (19) on the flow of rubber latexes gives the first data on the flow properties of pseudoplastics. Here the data obtained in the turbulent region could be properly correlated on the usual friction factor plot by using the viscosity at infinite shear, or the slope of the asymptotic limit of the shear stress, rate of shear diagram for a pseudoplastic in the laminar flow region.

Based on this work, MacLaren and Stairs (9) measured the viscosity of the Filter-Cel suspensions investigated in (19) by measuring the pressure drop in known sizes and lengths of pipe. By comparing the values thus obtained for Filter-Cel to those for water in the same pipes, it became possible to obtain a value of the viscosity similar to the turbulent viscosity defined by Binder and Busher (4).

In 1949, G. E. Alves (1) presented a summary of much of the available knowledge on the Flow of non-Newtonian Suspensions. Shear diagrams for several types of

Newtonian and Non-Newtonian suspensions, flowing in pipe are presented as well as a number of references to the work of the more significant investigators in the field.

The available information on heat transfer to suspensions of the solids in liquids is rather limited. Heat transfer coefficients of dilute suspensions of Filter-Cel in a concentric pipe heat exchanger were investigated by MacLaren and Stair (9). The conductivity of the suspending material, in their case, water, was used to correlate their data and the specific heat calculated on a weight fraction basis. Apparent viscosities in the turbulent range were calculated from the pressure drops in a straight length of pipe. In correlating their data, MacLaren and Stairs found that the points obtained at the high Reynolds numbers, agreed closely with the correlation for water alone. At low Reynolds numbers, the points for the slurry and water diverged. At Reynolds numbers lower than 40,000, it was found that a film of the Filter-Cel was baked on the heating surface. At the higher flow velocities, the slurry moved through the heating section fast enough to avoid the formation of a deposit.

Hoopes (11) data on the cooling of 0- 21 percent Filter-Cel slurries were found to agree within 10% with the Dittus-Boelter equation with the 0.4 exponent for the

Prandtl number. For the data of MacLaren & Stair on the same slurries the Reynolds number exponent of the Dittus Boelter equation had to be changed from 0.8 to 0.705 and the constant from 0.0225 to 0.0365. Both Hoopes et al. and MacLaren & Stair present their slurries as showing Bingham body flow, though MacLaren & Stairs did notice some manifestation of variation of this behavior at low fluid flow rates.

Shandling (16) investigated the heat transfer coefficients to aluminum-water slurries. Like the previously referenced investigator (9) he obtained his data in a steam jacketed heat exchanger which was a component part of a re-circulating system. Concentrations of slurry varied from .8 to 7.4%; the Reynolds numbers ranged from 20,000 to 100,000. It was determined that the heat transfer coefficients were not significantly affected with increase in the suspension concentration. A rise in viscosity at low velocities and higher concentrations was found to offset increases in the slurry conductivity. No correlation of the heat transfer coefficients of the suspensions could be made because of particle characteristics which could not be determined. Correlation of $Nu/Pr^{0.4}$ versus $Re^{.7}$ as indicated by the Dittus-Boelter equation gave a series of parallel lines having different ordinate intercepts. The same slope as the line for water data, i.e., 0.7 was obtained.

Bonilla et al. (6) investigated the heat transfer properties of chalk-water slurries at different concentrations. They found that the cooling of 0 to 21% slurries agrees within 10% with the Dittus-Boelter equation:

$$(hD/K_o) = 0.023\ (DG/U)^{0.8}\ (C_u/K_o)^{0.4} \qquad \text{Eq. (5)}$$

over a Reynolds number range of 3,000 to 230,000. Best agreement was obtained by using the following values: for K, the thermal conductivity of water, for C, the computed additive specific heat of the slurry and for u, the viscosity of the slurry was measured in the Wilhelm and Wroughton viscometer. A correlation between viscosities of the slurry and water was made with the Hatschek equation:

$$\text{Eq. (6)} \quad u_b = u_w / 1 - \phi^{1/3}$$

where u_b = bulk viscosity of slurry

u_w = viscosity of water

ϕ = volume fraction of solid in suspension

With the properties of the system evaluated in the above manner, the Reynolds, Prandtl, and Nusselt numbers were determined. After plotting $Nu/Pr^{1/3}$ versus Re, with percent solid as a parameter, it was shown that the $Nu/Pr^{1/3}$ value varied inversely with

concentration of solid and that the effect was more apparent in the lower Reynolds number range. The decrease in $Nu/Pr^{1/3}$ was found to be approximately a linear function of the solid concentration in the suspension.

Salamone (15) in 1954 completed a series of experiments with a number of suspensions consisting of various powdered solids in water. In this investigation, the variables investigated are the individual properties of the suspension's components with the exception of viscosity, velocity, and density which are measured as bulk properties based upon the conditions of heat transfer. The experimental data is so correlated to yield the exponents of equation (2) by dimensional analysis. Another correlation assumes that existing relationships for liquids apply to suspensions, providing that the pertinent properties may be evaluated for the suspension. Evaluation of all properties except the effective thermal conductivity of the suspension could be made. Calibration of the experimental equipment with water resulted in calculation of the effective thermal conductivity of the suspension. The latter was then correlated with the thermal conductivities of the solid, the liquid and the concentration and particle size of the solid. This investigator chose the turbulent flow region for his work to develop high coefficients of heat transfer and

to minimise the problem of settling of the solid particles in the piping system.

Orr and Dallavalle (15) worked with various suspensions of powdered solids in water and ethylene glycol. The equation:

$$\mu_b = \frac{\mu}{(1 - \frac{\phi}{\phi'})\ 1.8} \qquad \text{Eq. (7)}$$

was used to calculate the suspension viscosity. ϕ' is the volume fraction of the solid in a sedimented bed. Experimental measurements with a Saybolt type viscosimeter gave results which agreed closely with the above referenced equation. Calculation of the thermal conductivities of the suspensions agreed rather well with the conductivities determined experimentally. The data obtained were correlated rather well with the use of the Dittus-Boelter equation as modified by Sieder and Tate (20).

$$\frac{hD}{k} = 0.027 \left(\frac{DG\rho}{\mu}\right)^{0.8} \left(\frac{C\mu}{k}\right)^{1/3} \left(\frac{\mu}{\mu_w}\right)^{0.14} \qquad \text{Eq. (8)}$$

Heat transfer characteristics of non-Newtonian solution (single fluid phase) were investigated by Chu et al. (8). Heat transfer correlations for ordinary liquids were found to apply as long as the proper viscosity and thermal conductivity were used for the solution.

DESCRIPTION OF APPARATUS

A schematic diagram of the apparatus which is similar to that constructed by Bonilla (6) and Salamone(15) was assembled for the purpose of obtaining the data for this investigation as shown in Figure 1 .

The slurry was prepared and stored in a 55 gallon drum provided with a "Lightning" motor-driven agitator. A Worthington pump of adequate capacity, driven by a 1-1/2 H.P. 220V, 60 cycle A.C. motor at 3450 RPM transported the slurry from the storage tank, through a by-pass, which was installed to insure positive rate control and thorough mixing by recycling slurry back into the tank, and then thru the system back to the tank.

The circulatory system consisted of a heat transfer section for transfer measurements, two cooling sections consisting of a concentric pipe heat exchanger located after the heating section which kept the slurry in the viscometer (which came after the cooling exchanger) at the average temperature of the slurry in the heating section; the second section consisted of 100 feet of close wound 1/2" copper tubing in the slurry storage tank which maintained the slurry feeding the system at isothermal conditions.

All lines in contact with the slurry were 85-15 brass, except as noted above.

The heat transfer section contained a 1/2 inch I. P.S. brass pipe inside a 1-1/4 inch wrought iron pipe which in

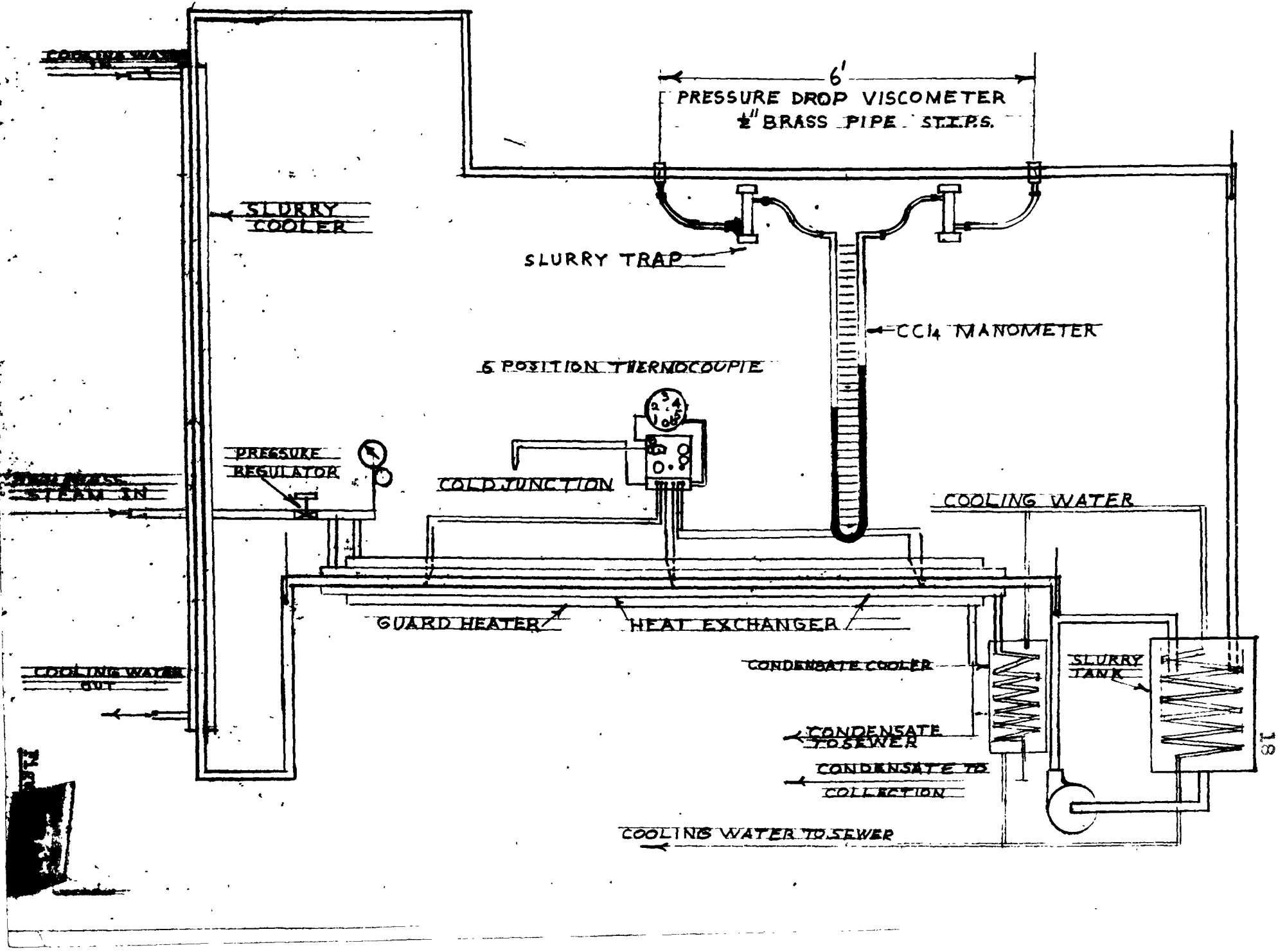
6'
PRESSURE DROP VISCOMETER
½" BRASS PIPE S.I.P.S.
SLURRY COOLER
SLURRY TRAP
CCl_4 MANOMETER
6 POSITION THERMOCOUPLE
PRESSURE REGULATOR
COLD JUNCTION
COOLING WATER
GUARD HEATER
HEAT EXCHANGER
CONDENSATE COOLER
SLURRY TANK
CONDENSATE TO SEWER
CONDENSATE TO COLLECTION
COOLING WATER TO SEWER

Figure 2

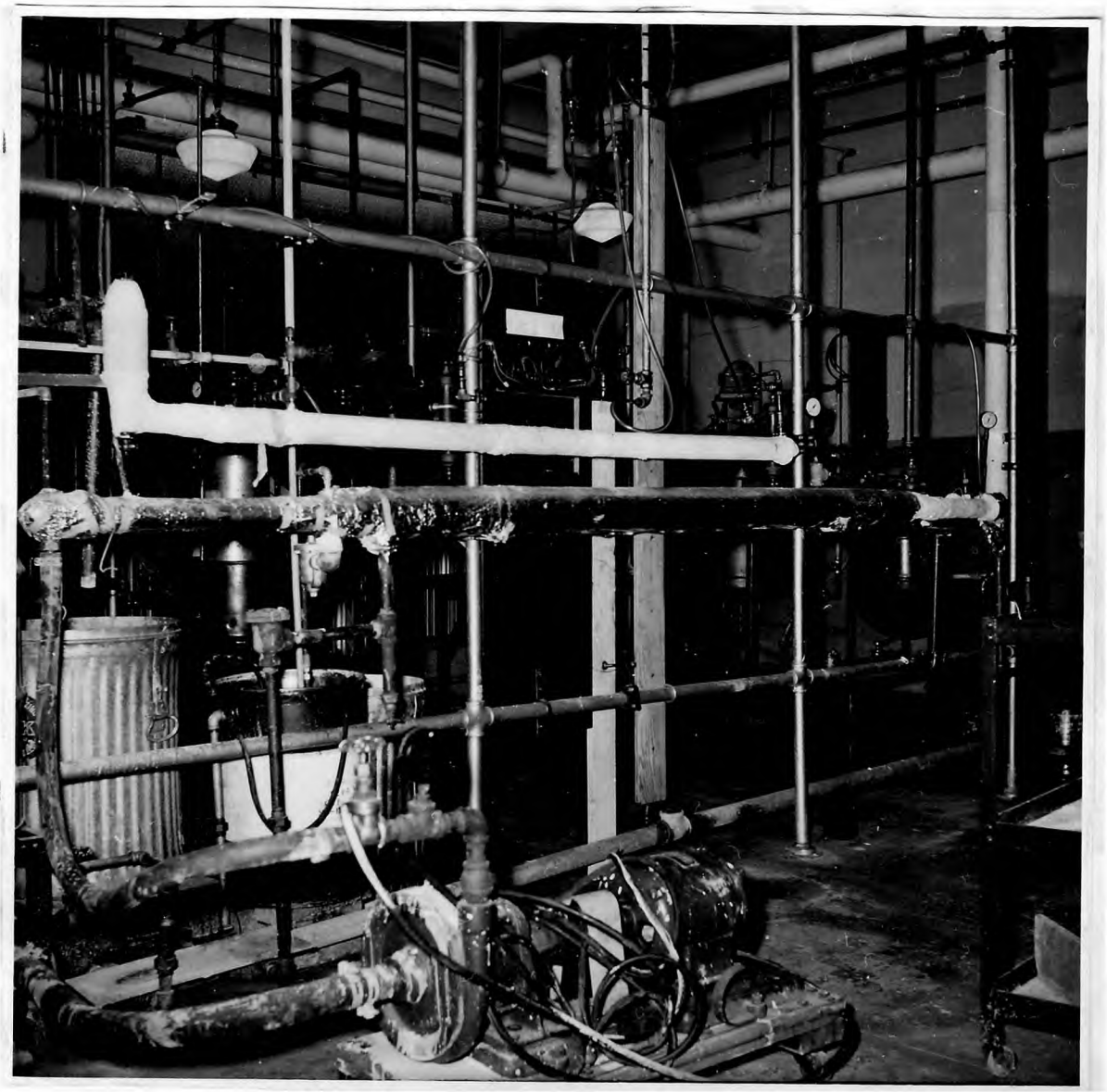

Front View of Apparatus

Showing

Heating, Cooling, Pressure Drop, and Calming Sections

Figure 3

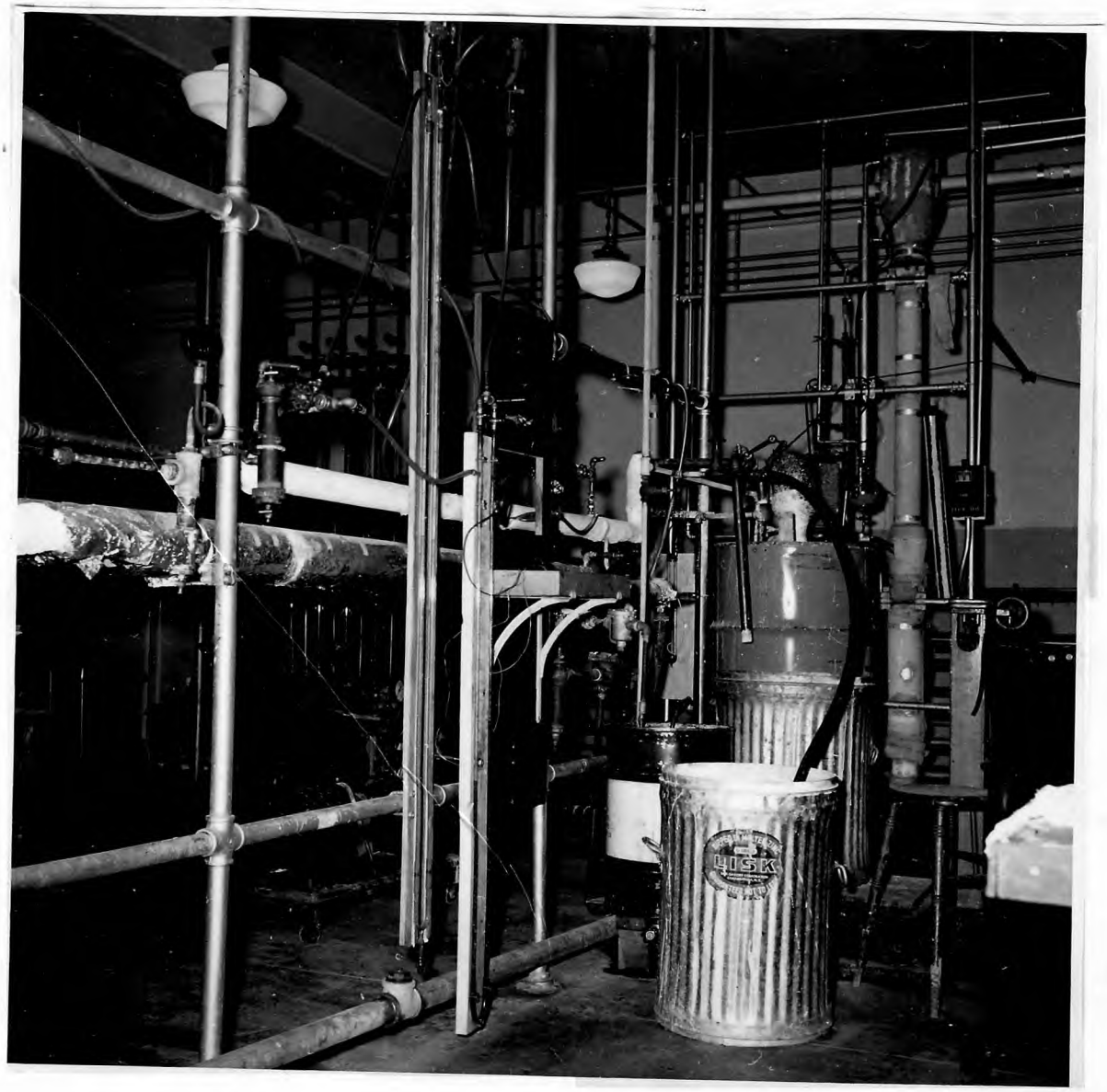

Rear View of Apparatus Showing Slurry, Condensate and Slurry Sample Storage Containers, Thermocouple Rotary Selector Switch, Potentiometer Platform, Manometers, and Slurry Traps.

turn was surrounded by a 2-1/2 inch wrought iron pipe.[21] Steam was circulated through both annular spaces, the outer serving as a guard heater. Iron tees and bushings located at the ends of the 2-1/2 inch and 1-1/4 inch pipe provided the inlet and outlet for the steam in both annular sections. Sealing of the outer annulus was accomplished by screwing 2-1/2 x 1-1/2" reducing bushings into the 2-1/2" tees and inserting the 1-1/4 inch pipe which was then welded to the bushings. Sealing of the inner annuli was accomplished with the aid of reducing bushings, close nipples, and unions which were turned down inside and packing added to serve as a packing gland at each end. (Fig. 1). Air vents were provided at each end of the inner annulus.

Heating of the slurry was accomplished in the 1/2" pipe by steam flowing in the inner annulus counter current to experimental solution over a length of 8 feet. Provision was made for collecting and weighing the condensate obtained from the inner annulus. The 12 foot length of the inner 1/2 inch pipe provided for a calming section of approximately 2 feet at each end. Each end was connected to a 1" tee containing a thermometer well in which oil was used as a heat transfer medium. The thermometers used to record the inlet and outlet slurry temperatures were graduated in 1/10°C and ranged from -1° to 101° C. Brass flanges with rubber gaskets were installed between the ends of the 1/2 inch pipe and the thermometer well tees to minimize end effects due to heat conduction between the heating section and the rest of the apparatus.

The thermocouples were installed in the 1/2 inch brass pipe in the following manner: Three grooves were cut into the pipe wall at either end with the aid of a milling machine. Four of these were made 18 inches long, two commencing approximately 12 inches from either end of the 1/2 inch brass pipe. The third commencing at the same point as the others on both ends was extended over to the center of the 1/2 inch pipe. The grooves were wide enough to accommodate a set of copper-constantan thermocouple wires No. 22 gauge. The thermocouple junction was positioned into the groove and the latter filled with molten solder. The solder was smooth and polished with emery cloth until the surface was uniformly circular. The thermocouple wire was snugly positioned along the length of the grooves and some litharge cement with glycerin (5) was used to fill the remaining volume within the grooves. The entire pipe surface was polished smooth with fine emery paper. In all, six copper-constantan thermocouple junctions were attached to the outer surface at the top and bottom near the ends and the center of the inner annulus. A drawing of the thermocouple installation is shown in Figure 1.

The wires for three of the thermocouples at each end were taped to the 1/2 inch inner brass pipe and surrounded with individual strands of plastic translucent tubing for protection. This provision was made for the length of wire extending from the 1/2 inch pipe out to a terminal block adjacent to a rotary selector switch. In addition to the

use of a strand of plastic tubing for each set of thermocouple wires, a larger size of plastic tubing was used to contain all three of the individual thermocouples at each end.

The thermocouple wires, contained within the plastic tubing, were connected to a terminal block and from this point connected through a rotary switch to a Leeds Northrup portable precision potentiometer. An ice bath was used as a reference junction.

The heating section was completely insulated with 85% magnesia pipe insulation and aluminum foil. The cooler was a double pipe type heat exchanger consisting of 1 inch brass I. P.S. pipe inside a 2 inch standard iron pipe. Cold water was circulated counter-currently to the slurry through the annular space.

The viscometer consisted of an insulated 1/2 inch I.P.S. brass pipe with pressure taps spaced 6 feet apart. A 2 foot long calming section preceded the pressure drop section. Approximately 30 inches beyond the pressure drop section provision was made for a tee containing a thermometer well. A carbon tetrachloride manometer was used to determine pressure drop data. Traps were installed just after the pressure traps to prevent slurry particles from reaching the manometer lines. Lines to and from the traps were made of transparent Excelon plastic tubing. This provision enabled viewing air or solid material which occasionally found its way into the manometer lines. The manometer was so built that the traps

and transparent lines could be conveniently flushed with water. This was done before all readings to remove sediment and air from the lines and traps.

The pipe returning to the slurry tank was provided with a set of quick opening valves to conveniently allow diverting the slurry into a weighing tank for flow rate measurements. A cooling coil was provided in the slurry tank to maintain isothermal conditions in the tank.

The solids used for the slurries are described in Table 1 .

EXPERIMENTAL PROCEDURE

The apparatus was first operated with water and the data used to plot Figures 5 and 6. The data for Figure 6 was obtained from the pipe line viscometer and shows excellent agreement with the line obtained from the von Karman equation $\frac{1}{\sqrt{f}} = (2 \log Re \sqrt{f}) - 0.8$ Eq. (9) as shown by the broken line below it. The heat transfer data gave a line with the same slope as the accepted data (Figure 5) although the intercept was greater. Four additional water runs were made to check the von Karman plot. For these runs the heat transfer data was not taken. This data agreed well with the first ten runs.

After the water runs had been shown to be acceptable the slurry runs were started. For each set of runs about forty gallons of water were run into the slurry tank and the pump started to circulate it through the system. The Lightning mixer was turned on and sufficient solid was added to five approximately the weight percent of solid desired.

The steam and cooling water to the cooling section, the helical copper coils in the slurry tank and the condensate cooling tank were then turned on. The slurry rate was set by manipulating the pump discharge valve in

conjunction with the by-pass valve to give the approximate desired rate as shown by the pressure drop differential on the manometer in the pipe line viscometer. When steady state was reached as evidenced by constant temperature readings of the slurry at the inlet and outlet of the heat exchanger and in the viscometer for a period of ten minutes or more, the above, the thermocouple millivolts, the manometer differential, and the steam pressure were observed and recorded. The inlet temperature, outlet temperature and manometer differential were averaged over the last two or three readings, if there was a variance, to minimize the effect of small fluctuations. The steam rate was determined by weighing a sample collected over a known period of time. The slurry flow rate was determined by diverting the flow to the slurry tank into a tared tank on a portable platform scale and weighing the contents collected over a known period of time. At least seventy-five pounds of slurry were collected to minimize the error in the determination. A pair of quick opening valves insured rapid change over from flow to the slurry tank to flow to the tared tank and vice-versa.

The density of the suspension was obtained by weighing four liters of the slurry in a flask in which the same volume of water had previously been weighed at the same temperature. This density was in turn used to determine

the weight-fraction of solid in the slurry from previously prepared curves based on known concentrations. These curves which are illustrated in Figures 4 and 4A were prepared by weighing a clean dry volumetric flask. It was then filled to the graduated mark with water and weighed accurately. The water was poured out and about two grams of solid added and weighed after which the flask was again filled with water leaving the solid in the flask. By subtracting the tare weight of the flask from both the weight of the flask plus the water alone and the weight of the flask plus the water and the solid, the density was found by dividing the latter by the former. The weight fraction was determined from the weight of the solid and the weight of the solid-water mixture. This procedure was continued with four samples of each solid at steps of two grams, five grams, ten grams and fifteen grams shown in Table No. 2, and a plot of density versus weight fraction was made.

TABLE 1

Source of Materials and Their Physical Properties

Material	Source	Density at 20°C gm/cc	SP. Heat 60°C BTU/#°F.	Therm. Conduct. BTU/hr °F/ft²/ft	Av.Part Size - Microns
Atomite Chalk Powder	Thompson Weinman & Co. Montclair, N.J.	2.71 (Co.)	0.209 Perry	0.40 Perry	2.5 (Co.)
Snow Flake White Powder	Thompson Weinman & Co. Montclair, N.J.	2.71 (Co.)	0.209 Perry	0.40 Perry	6 (Co.)
No. 1 White Powder	Thompson Weinman & Co. Montclair, N. J.	2.71	0.209 Perry	0.40 Perry	14
Copper Powder	Charles Hardy, Inc. New York, N.Y. Electrolytic Cir. Powder	8.92 Perry	0.0932 Perry	220 Perry	30 **

All properties of water from Perry

Thermal conductivity of brass (85015 red brass)

90 BTU/hr°F/ft²/ft

** As calculated from size distribution data supplied by manufacturer

TABLE 2

Density-Weight % Data

Solid	Wt. Solid in 100 cc of Slurry grams.	Total Wt. of 100 cc Slurry gm/cc	Temp. °C	Wt. % Solid	Slurry Density gm/cc
Atomite	2	100.62	26	1.9	1.007
	5	102.47	26	4.9	1.026
	10	105.72	26	9.5	1.059
	15	109.2	26	13.7	1.094
Snowflake White	2	100.7	25	2	1.008
	5	102.4	25	4.9	1.025
	10	105.7	25	9.4	1.058
	15	108.5	25	14.2	1.066
No. 1 White	2	99.73	25.5	2	.9988
	5	102.63	25.5	4.8	1.028
	10	105.63	25.5	9.4	1.058
	15	108.53	25.5	13.8	1.087
Copper				1.411	1.00
				3.35	1.02
				6.41	1.05
				10.75	1.095
				13.99	1.124

DENSITY VS WEIGHT FRACTION CURVES

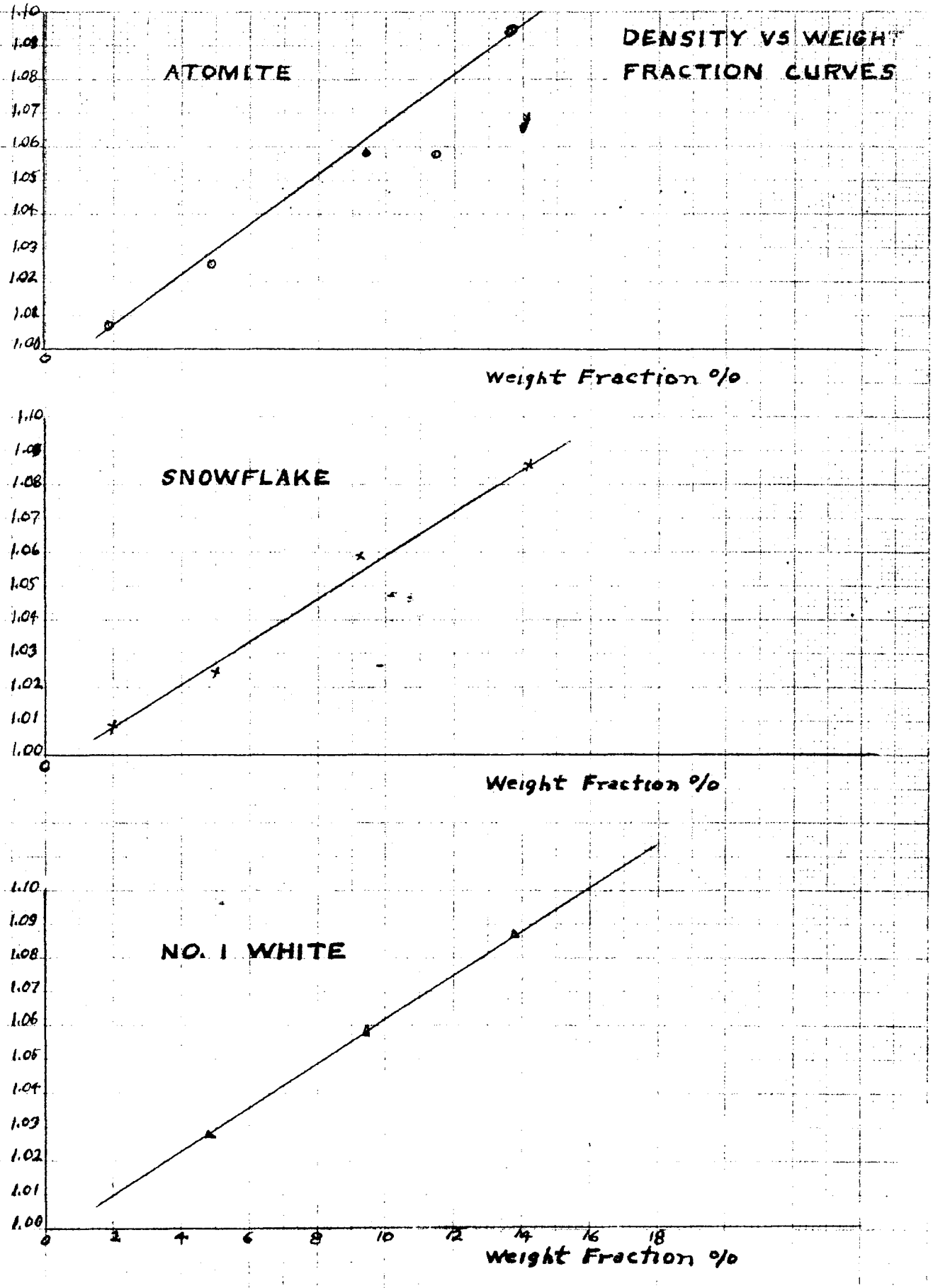

Fig. 4

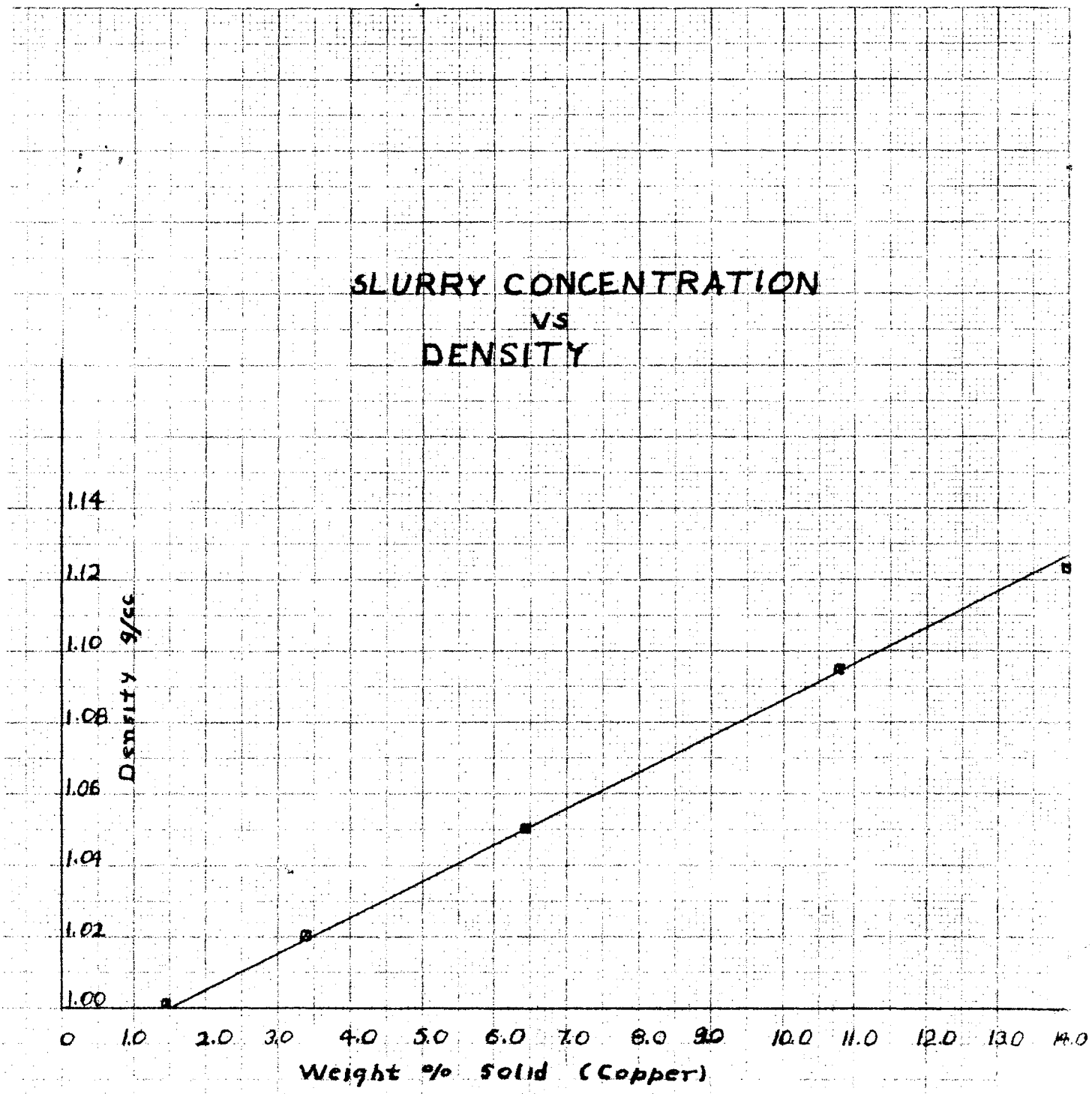

Taken From J.J. Salamone

Fig. 4A

TABLE NO. 3
Observed Data
Water Calibration Run

Run No.	1	2	3	4	5	6	7	8	9	10	11	12	13	14
Inlet Temperature, °C	33.3	47.7	46.2	44.0	40.8	33.7	31.5	23.6	38.8	43.5				
Outlet Temperature, °C	78.2	75.1	75.0	76.3	75.5	74.3	76	73.5	78.1	78.1				
Average Temperature, °C	55.8	61.4	60.6	60.2	58.2	54.0	53.8	48.6	58.5	60.8				
T. C. #1, m.v.	4.55	4.4	4.52	4.5	4.22	4.36	4.41	4.62	4.51	4.6				
T. C. #2, m.v.	4.34	4.05	4.16	4.1	3.86	4.15	4.28	4.62	4.16	4.05				
T. C. #3, m.v.	4.15	3.82	3.85	3.9	3.86	4.03	4.11	4.62	4.09	3.94				
T. C. #4, m.v.	4.45	4.28	4.41	4.39	4.33	4.43	4.39	4.62	4.54	4.44				
T. C. #5, m.v.	4.67	4.55	4.6	4.58	4.55	4.54	4.55	4.62	4.74	4.67				
T. C. #6, m.v.	4.36	4.30	4.33	4.39	4.39	4.46	4.45	4.62	4.6	4.56				
Aver.Thermocouple Temp., °F	217.5	212.1	213.3	213.2	209	213.9	215.4	225.2	218.2	217.4				
Viscometer Temp., °C	58.3	64	63	63	59.8	55.1	55	46.2	60.1	62.7	18	19.2	20.8	22
Water Mass Rate, lbs./min	28.75	81	70.5	58.5	49.5	50.75	25.8	12	40.3	53.5	53	38.5	30.13	18.2
Condensate Mass Rate, lbs./min	3.1	4.25	4.25	4.0	3.72	2.91	2.65	1.46	3.42	3.93				
Manometer Read.Inches CCl/4	9.75	62	51.3	37.63	27.75	13.81	9	3.125	19.19	32.06	37.56	21.38	13.63	5.63
Steam Pressure, psig	7.2	6.5	6.6	7	6.1	6.5	6	7.1	7.6	7.9				

TABLE NO. 4

Calculated Data
Water Runs

Run No.	1	2	3	4	5	6	7	8	9	10	11	12	13	14
Friction Factor, f	.0204	.0165	.0180	.0192	.0198	.0236	.0235	.0340	.0206	.0196	.0233	.0252	.0263	.0297
$1/\sqrt{f}$	6.96	7.90	7.46	7.20	7.11	6.50	6.51	5.14	6.95	7.14	6.54	6.29	6.17	5.80
Re $\sqrt{f}$	5,220	14,340	12,980	11,080	9,040	5,560	4,760	2,434	7,550	10,100	4,670	3,650	3,040	2,010
Reynolds No.,Re Heat Sec.	36,300	111,700	96,600	79,800	64,200	37,100	31,000	12,500	52,500	72,100	30,600	23,000	18,800	11,700
Water Viscosity, cp	0.483	9.443	.445	.448	.470	.505	.507	.585	.468	.453				
Pipe Wall Temp.Drop t_m ^oF	9.2	15.9	15.1	13.4	12.3	8.8	8.2	4.3	11.3	13.3				
Inside Pipe Wall Temp.t_{si} ^oF	208	196	198	200	197	205	207	221	207	204				
Log Mean Temp.Dif. t_{lm} ^oF	68.0	49.5	54.2	54.0	54.0	69.6	71.0	94.4	63.0	56.9				
Water Heat BTU/hr x 10^3	139	240	227	202	186	135	124	64.8	171	200				
Steam Heat BTU/hr. x 10^3	178	244	244	234	218	171	152	83.8	196	227				
Film Coeff. BTU/hr.ft^2 ^oF	1570	3740	3220	2880	2650	1493	1346	528	209	270				
Nusselt Number, N	215	512	441	394	362	204	184	72.3	28.6	36.9				
Prandtl Number,P Visc.Sec.	3.10	2.84	2.86	2.87	3.02	3.24	3.25	3.75	3.01	2.9				
p 0.04	1.57	1.52	1.52	1.52	1.56	160	1.60	1.70	1.55	1.53				
N/p 0.04	137	338	289	258	233	128	115	42.6	18.4	24.1				

COMPARISON OF EXPERIMENTAL HEAT TRANSFER DATA FOR WATER WITH OTHER WATER DATA

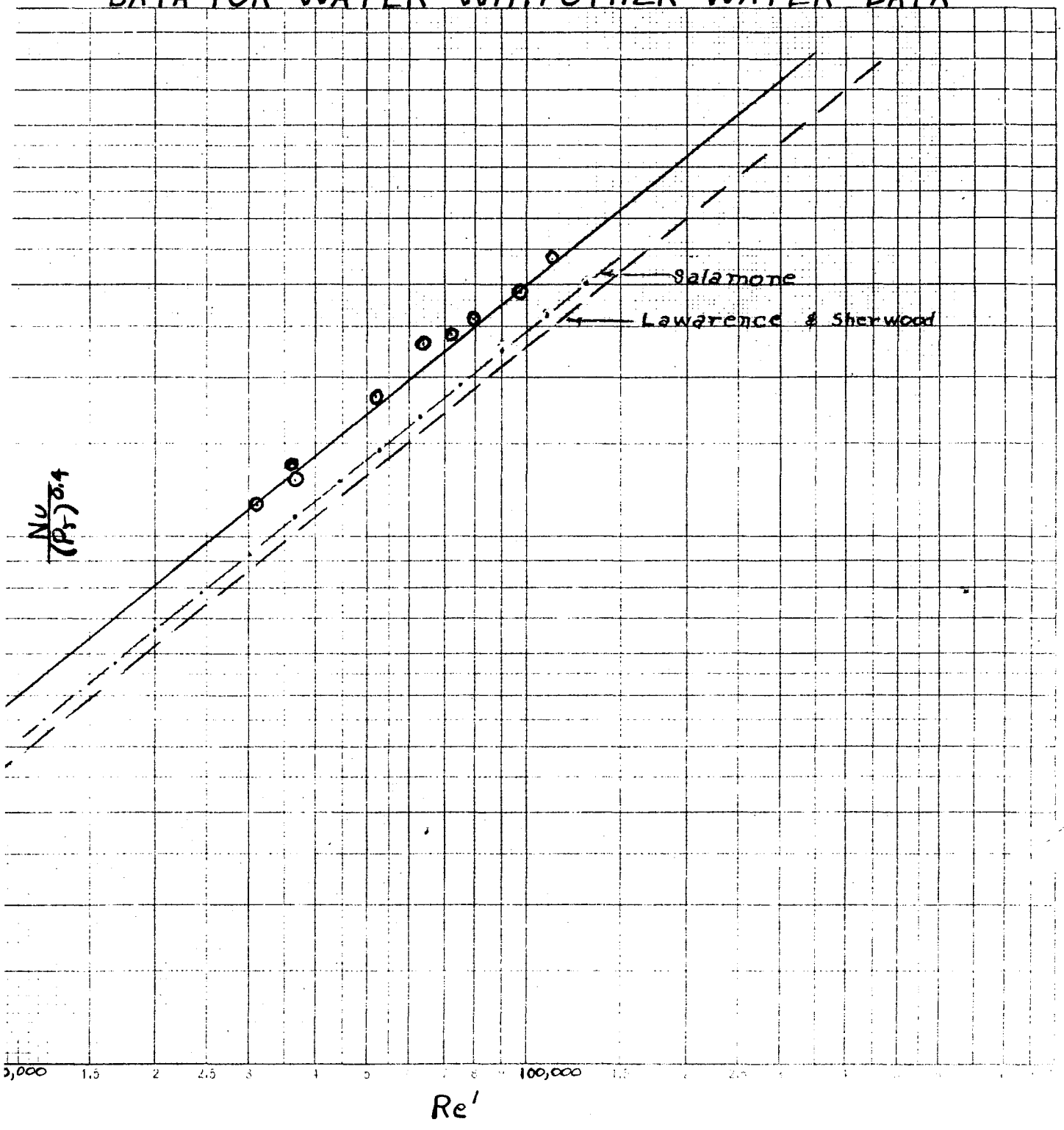

Fig. 5

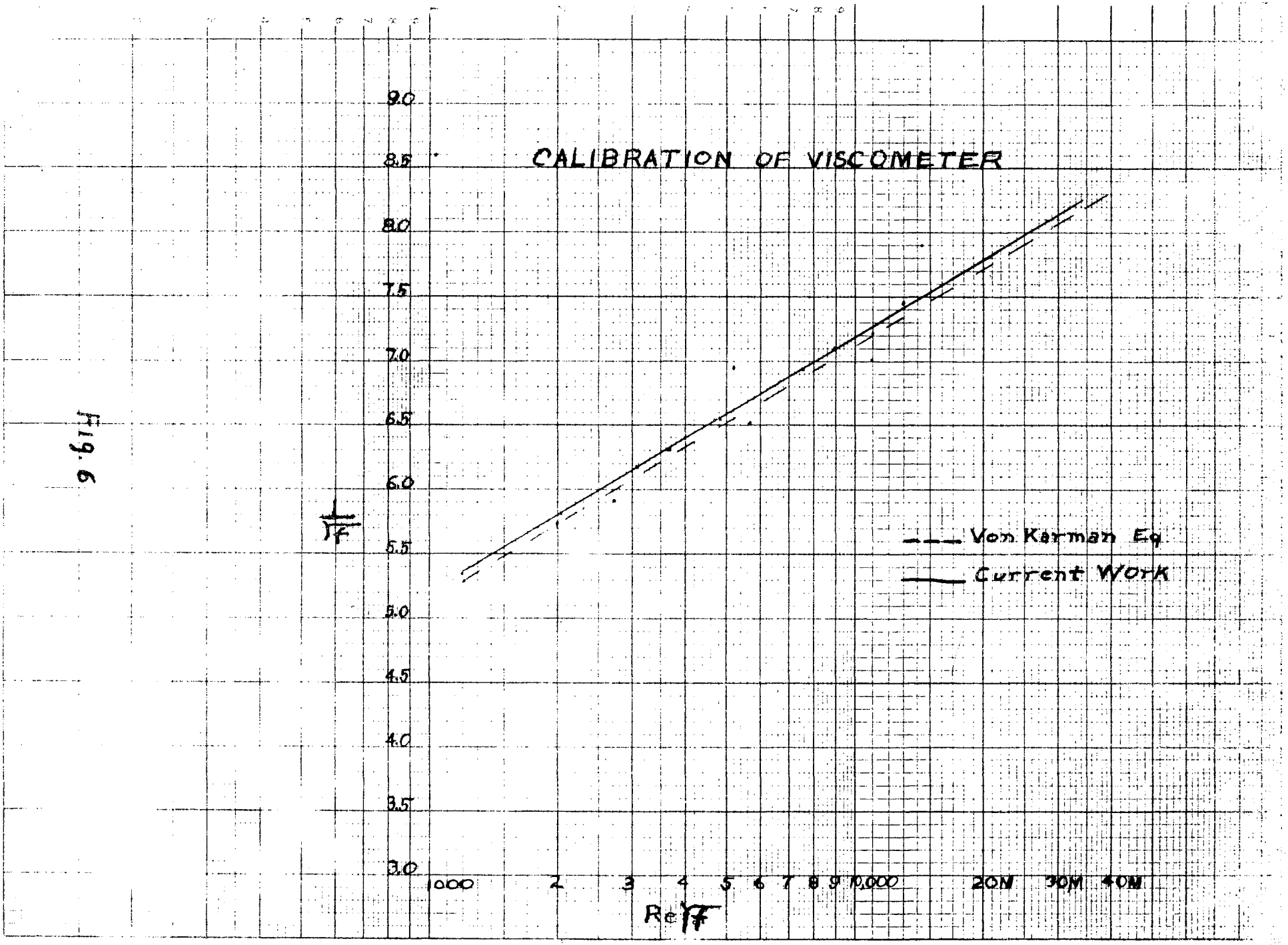
CALIBRATION OF VISCOMETER
9.0
8.5
8.0
7.5
7.0
6.5
6.0
5.5
5.0
4.5
4.0
3.5
3.0
1/√f
Von Karman Eq
Current Work
1000
2
3
4
5
6
7
8
9
10,000
20M
30M
40M
Re√f

Fig. 6

TABLE NO. 5

Observed Data
Atomite Slurry Run

	1	2	3	4	5	6	7	8	9	10	11	12
Inlet Temperature, ^{o}C	38.0	41.0	37.4	32.8	37.0	39.6	41.6	40.1	39.3	38.3	34.2	
Outlet Temperature, ^{o}C	65.7	67.8	72.5	74.3	70.6	72.1	72.3	74.3	75.8	78.1	80.7	
Average Temperature, ^{o}C	52.0	54.4	55.0	54.6	54.0	55.8	57.9	58.7	59.6	60.5	59.5	
T. C. #1, m.v.	3.55	3.54	3.81	3.91	3.80	3.72	3.76	3.87	3.93	4.05	4.16	
T. C. #2, m.v.	3.57	3.55	3.81	3.91	3.80	3.76	3.90	4.1	4.00	4 .16	4.29	
T. C. #3, m.v.	3.60	3.55	3.73	3.73	3.62	3.65	3.70	3.73	3.75	3.87	4.05	
T. C. #4, m.v.	4.22	4.37	4.38	4.27	4.29	4.31	4.45	4.45	4.45	4.55	4.60	
T. C. #5, m.v.	4.42	4.51	4.59	4.49	4.57	4.65	4.86	4.81	4.81	4.85	4.89	
T. C. #6, m.v.	4.27	4.36	4.47	4.49	4.57	4.65	4.82	4.81	4.74	4.80	4.80	
Aver.Thermocouple,Temp.^{o}F	198.9	200.2	206.4	206.8	205.4	205.8	210.5	212.7	212.1	217.6	219.8	
Viscometer Temp., ^{o}C	52.0	54.8	56.0	53.5	53.8	55.8	57.0	57.2	57.6	58.2	57.4	
Water Mass.Rate,lbs/min.	47.75	57.60	30.60	23.10	38.60	45.62	51.75	41.25	37.60	31.30	21.25	
Condensate Mass Rate, lbs/min.	2.77	3.02	2.66	2.06	2.68	2.93	3.16	2.81	2.54	2.36	1.95	
Manometer Read. Inches CCl_4	28.56	34.63	15.94	8.13	18.63	23.88	31.13	20.88	17.50	13.25	7.75	
Density, lbs/Ft^3	64.6	63.9	63.6	63.6	63.5	63.3	65.1	65.2	65.2	65.3	65.4	
Steam Pressure, psig	8.2	10.3	10.6	8.13	9.4	11.3	11.2	10.0	10.2	10.5	9.6	

TABLE NO. 6
Observed Data
Snow Flake

Run No.	1	2	3	4	5	6	7	8	9	10	11	12
Inlet Temperature, °C	45.3	45.3	42.6	42.0	38.8	34.3	33.9	37.4	41.3	43.3	45.5	48.1
Outlet Temperature, °C	76.0	77.2	77.6	80.4	80.2	84.2	81.5	80.7	82.1	79.9	78.4	79.0
Average Temperature, °C	55.6	61.2	60.1	61.2	59.5	59.2	57.7	59.1	61.7	61.6	62.0	63.6
T. C. #1, m.v.	3.65	3.79	3.81	3.92	4.00	4.22	4.22	4.01	4.07	3.90	3.85	3.85
T. C. #2, m.v.	3.66	3.77	3.92	4.05	4.07	4.22	4.27	4.07	4.23	4.07	3.93	3.96
T. C. #3, m.v.	3.58	3.68	3.68	3.84	3.83	4.03	4.02	3.85	3.96	3.88	3.77	3.75
T. C. #4, m.v.	4.38	4.39	4.40	4.54	4.51	4.52	4.60	4.47	4.65	4.55	4.45	4.48
T. C. #5, m.v.	4.74	4.75	4.73	4.85	4.73	4.77	4.78	4.74	4.98	4.86	4.81	4.83
T. C. #6, m.v.	4.61	4.66	4.65	4.74	4.69	4.73	4.73	4.68	4.89	4.76	4.70	4.69
Aver.Thermocouple Temp.°F	205	208	209	214	213	217	218	213	219	214	211	211
Viscometer Temp., °C	58.5	59.1	59.1	60.0	58.1	57.0	57.2	59.0	62.0	62.0	62.7	64.2
Water Mass.Rate, lbs/min.	56.7	48.5	43.5	35.7	28.6	17.2	20.3	27.7	35.1	42.4	50.6	56.1
Condensate Mass Rate,lbs/min.	3.44	2.91	2.79	2.58	2.37	1.85	2.00	2.44	2.87	3.03	3.23	3.36
Manometer Read.Inches, CCl_4	34.2	27.8	22.1	15.7	10.6	5.1	6.9	10.5	15.4	21.0	28.5	34.0
Density, lbs/Ft^3	64.0	64.0	64.0	64.0	64.0	64.0	66.3	66.3	66.3	66.3	66.3	66.3
Steam Pressure, psig	10.0	9.2	9.8	10.8	9.5	10.2	9.5	9.5	12.5	10.5	9.1	9.6

TABLE NO. 7
Observed Data
No. 1 White Slurry Runs

Run No.	1	2	3	4	5	6	7	8	9	10
Inlet Temperature, °C	44.1	44.0	44.0	41.9	38.1	46.2	41.1	42.2	38.5	36.1
Outlet Temperature, °C	77.7	79.8	80.5	81.1	84.6	78.1	76.4	82.1	83.2	83.0
Average Temperature, °C	60.9	61.9	62.3	61.5	61.4	62.2	58.8	62.2	60.9	59.5
T. C. #1, m.v.	3.63	3.79	3.77	3.81	4.22	3.79	3.77	3.97	4.10	4.14
T. C. #2, m.v.	3.68	3.79	3.77	3.86	4.10	3.72	3.77	3.97	4.10	4.14
T. C. #3, m.v.	3.68	3.73	3.73	3.82	3.96	3.66	3.61	3.90	4.02	4.01
T. C. #4, m.v.	4.50	4.51	4.49	4.52	4.53	4.45	4.43	4.55	4.65	4.65
T. C. #5, m.v.	4.84	4.80	4.78	4.77	4.88	4.81	4.76	4.83	4.88	4.85
T. C. #6, m.v.	4.62	4.70	4.70	4.71	4.79	4.69	4.66	4.75	4.81	4.77
Aver.Thermocouple Temp. °F	209	210	209	211	217	208	208	214	218	218
Viscometer Temp., °C	57.6	58.0	58.1	57.5	56.2	59.0	56.5	59.5	58.3	57.0
Water Mass. Rate lbs/min.	47.6	42.1	39.6	34.0	25.1	54.0	44.3	35.4	26.6	22.8
Condensate Mass.Rate lbs/min.	2.77	2.83	2.62	1.99	2.40	3.20	2.83	2.50	2.20	1.97
Manometer Read.Inches CCl_4	28.6	22.6	20.5	16.5	9.3	33.5	23.9	15.0	9.69	7.25
Density - lbs/Ft^3	64.5	64.5	64.5	64.5	64.5	66.4	66.4	66.4	66.4	66.4
Steam Pressure, psig	9.75	9.90	9.20	8.6	10.1	10.3	9.2	10.4	10.2	9.5

TABLE NO. 8

Observed Data
Copper Slurry

Run No.	1	2	3	4	5	6	7	8	9	10	11	12	13	14	15	16
Inlet Temperature, °C	44.7	44.0	40.5	36.3	38.9	36.2	33.6	46.9	47.3	40.8	44.3	35.5	31.6	43.1	46.0	36.7
Outlet Temperature, °C	77.8	81.4	81.4	82.0	82.9	83.9	83.9	88.9	84.6	92.2	88.1	87.9	87.6	81.7	81.0	85.2
Average Temperature, °C	61.3	62.2	61.0	59.2	60.9	60.1	58.8	67.9	66.0	66.5	66.2	61.7	59.6	62.4	63.5	61.0
T. C. #1, m.v.	3.64	3.90	3.93	3.86	3.75	3.95	4.10	3.80	3.60	4.09	3.82	3.63	3.67	3.92	3.78	3.85
T. C. #2, m.v.	3.64	3.85	4.86	3.86	3.89	4.10	4.25	4.05	3.82	4.23	4.05	3.75	3.67	3.95	3.81	3.88
T. C. #3, m.v.	3.70	3.91	3.95	3.92	3.96	4.06	4.17	4.18	4.00	4.36	4.16	3.84	3.80	4.07	3.90	3.97
T. C. #4, m.v.	4.5	4.66	4.66	4.56	4.59	4.73	4.73	4.97	4.76	5.05	4.89	4.50	4.55	4.60	4.45	4.55
T. C. #5, m.v.	4.83	4.99	4.92	4.78	4.83	4.90	4.90	5.30	5.12	5.34	5.17	4.77	4.85	4.12	4.66	4.70
T. C. #6, m.v.	4.62	4.83	4.81	4.68	4.69	4.80	4.80	5.13	4.93	5.24	5.02	4.63	4.68	4.74	4.56	4.66
Aver.Thermocouple Temp. °F	207.0	215.0	214.5	211.5	212.3	217.8	220.3	223.0	215.8	228.1	221.0	222.3	225.5	202.3	208.5	212.0
Viscometer Temp. °C	62.6	64.3	61.9	58.4	61.1	57.0	54.6	64.4	63.0	61.7	63.0	57.0	53.1	60.0	61.3	57.8
Copper Mass.Rate #/min.	59.2	44.8	39.3	29.4	32.2	25.6	19.4	50.6	58.5	31.5	44.8	20.6	16.7	49.3	62.0	28.3
Condensate Mass Rate #/min.	3.29	3.37	3.07	2.58	2.75	2.31	2.07	4.06	4.22	3.43	3.81	2.39	1.93	3.43	3.07	2.69
Man.Reading Inches CCl_4	33.0	27.0	19.0	11.5	15.00	9.5	6.3	32.0	45.0	14.5	25.5	7.25	4.50	33.0	48.0	12.0
Density - lbs/FT^3	63.6	63.6	63.6	63.6	63.6	63.6	63.6	64.5	64.5	64.5	64.5	64.5	64.5	66.0	66.0	66.0
Steam Pressure - psig	10.0	12.2	10.7	9	9.4	11.8	10.3	19.8	16.0	18.3	17.3	12.5	11.0	9.6	11.3	9.0

EXPERIMENTAL RESULTS

The heat balances obtained were very poor, the condensate collected showing a higher heat input than the temperature rise of the slurry in almost all of the cases with the poorest agreement occurring at the lower mass rates. All of the heat transfer calculations were based on the temperature rise of the slurry and the average value of the calculated slurry heat capacity. Since there was good agreement between our data and published data of other investigators, it was decided not to stop the experimental work to make modifications of the apparatus to improve its performance. The pilot tube of the steam pressure reducing valve is connected to the low pressure side at the end of the header feeding steam to the heat section. It is possible for condensate to be forced into the pilot tube and make the steam pressure unsteady and unreliable. The pilot tube connection should be moved back from the end of the line and pitched away from the pressure reducing valve so that it drains dry and a steam trap should be installed at the end of the header to keep the steam as dry as possible. It is also recommended that a calorimeter be installed on the inlet steam to determine its quality.

The friction factor was calculated from the equation:

$$f = \frac{\Delta P \, D \, 2g_c}{\rho \, L \, V^2} \qquad \text{Eq. (10)}$$

The pressure drop was read from the pipe line viscometer which consisted of two pressure taps six feet apart connected to a carbon tetrachloride manometer. The density was determined by comparing the weight of equal volumes of slurry and water at approximately the same temperature and the velocity was calculated from the mass rate.

The reciprocal of the square root of the friction factor was used in the von Karman equation (Figure 6) to obtain a Reynolds number from which an apparent viscosity was calculated. This viscosity was calculated from data observed at the temperature in the pipe line viscometer and a correction based on the ratio of the viscosity of water at the heat section temperature to the viscosity of water at the viscometer temperature was applied. In most cases this was a small correction since the ratio of the heat transferred to the slurry in the heat section to the heat transferred from the slurry in the cooling section was very close to one. This corrected viscosity was used to find a corrected Reynolds number.

The film coefficient of the heat transfer to the suspension was calculated from the conventional equation:

$$L = q/A\,\Delta tm \qquad \text{Eq. (11)}$$

where q is the rate of heat transfer evaluated from the product of the slurry temperature rise, the mass rate and the calculated slurry specific heat; A is the inside

surface area of the heated pipe, and Δtm is the log mean temperature difference between the arithmetic average inside pipe wall temperature and the inlet and outlet slurry temperatures.

Using the values calculated above and constants taken from the literature, the Nusselt number and Prandtl number were calculated. These values plus the ratios of thermal conductivity of the slurry to the thermal conductivity of the water, the heat capacity of the slurry to the heat capacity of the water, and the inside diameter of the pipe to the average slurry particle size which were constant for each slurry concentration, were used to calculate the coordinates of Figures 7, 8, and 9.

Salamone (15) has presented a discussion of the magnitude of the possible error in his work and since the equipment, procedure, and slurries investigated are substantially the same, his 10% overall error is applicable to this report.

The results were plotted in Figures 7, 8, and 9. From the slopes of these plots the resulting equation becomes:

$$\frac{hD}{K_f} = 0.346 \left(\frac{DVP}{u'}\right)^{0.7} \left(\frac{C_f u'}{K_f}\right)^{0.72} \left(\frac{D_s}{D}\right)^{0.15} \left(\frac{C_s}{C_f}\right)^{0.35} \left(\frac{K_s}{K_f}\right)^{0.08} \quad \text{Eq. (12)}$$

Figures 10, 11, and 12 give an overall correlation of the data.

TABLE NO. 9

Calculated Data - Atomite Slurry Runs

Run No.	1	2	3	4	5	6	7	8	9	10	11	Run No.
Friction Factor, f	.0223	.0191	.0303	.0271	.0228							
$1/\sqrt{f}$	6.7	7.24	5.75	6.06	6.62	.0206	.0212	.0224	.0226	.0246	.0312	K_s/K_f
$Re\sqrt{f}$	5750	10600	1850	2700	5200	6.96	6.86	6.70	6.65	6.36	5.66	D_s Mic.
Reynolds No., RE	38600	76800	10600	16300	34400	7800	6900	5750	5400	3850	1680	C_s/C_f
Bulk Viscosity u_b, lbs/min. ft.	.0303	.0184	.0706	.0348	.0275	54100	47200	38600	36000	24500	9490	Ft^2/Ft^3
Corrected Bulk Viscosity, u'_b	.0303	.0185	.0718	.0342	.0275	.0206	.0268	.0262	.0256	.0313	.0350	$(C_s/C_f)^{.35}$
Corrected Reynolds No.($\times 10^2$)	386	765	10.4	176	344	.0206	.0264	.0255	.0248	.0302	.0531	C_p Slurry Av.
Mass Fraction, solid in slurry, x	.064	.050	.040	.040	.040	541	480	396	372	254	98	$P_{sl.}$ gm/cc
Temp.Drop across Pipe Wall, t_m °F	9.0	10.8	7.4	6.6	9.04	.053	.078	.078	.078	.080	.085	# Atomite/ft^3 Slurry
Inside Pipe Wall Temp., t_{si}, °F	189.9	189.4	199.0	200.2	196.4	10.4	10.7	9.5	9.24	8.36	6.61	h 1.67
Log Mean Temp.Difference, t_{lm}, °F	57.9	56.2	63.0	64.7	63.0	195.4	199.8	203.2	202.9	209.2	213.2	D 1.67
Slurry Heat, BTU/hr.($\times 10^3$)	135.5	162	112	100	136	57.8	61.3	61.3	61.5	65.8	69.8	$N/(Pr)^{.04}$
Steam Heat, BTU/hr. ($\times 10^3$)	159	173	152	118	153	156	161	143	139	126	99.8	C .667
Film Coefficient, BTU/hr.ft^2 °F	1800	2220	1367	1190	1660	167	180	160	145	135	111	u .667
Nusselt Number, N	246	304	187	163	227	2070	2020	1734	1740	1450	1100	$\{N/(pr)^{.04}\}$ 1.67
Prandtl Number, P	4.81	2.94	11.4	5.43	4.36	284	277	238	238	199	151	K_e
$p^{.72}$	3.00	2.13	5.50	3.27	2.80	3.27	4.19	4.05	3.94	4.79	8.43	$N/(Pr)^{.72}\left(\frac{D_s}{D_s}\right)^{.05}\left(\frac{C_s}{C_f}\right)^{.35}\left(\frac{K_s}{K_f}\right)^{.05}$
$N/P^{.72}$	82.0	143	34	49.8	81.1	2.28	2.73	2.66	2.61	2.99	4.45	
$Re^{.7}$	1720	2770	660	940	1591	124	101	89.5	91.2	66.5	53.9	$N/(Pr)^{.72}\left(\frac{D}{D_s}\right)^{.52}\left(\frac{C_s}{C_f}\right)^{.35}\left(\frac{K_s}{K_f}\right)^{.08}$
$N/P^{.72}\ Re^{.7}$	.0476	.0516	.0515	.0530	.0510	2160	1990	1740	1660	1270	650	
D/D_s	6260	6260	6260	6260	6260	.0574	.0507	.0514	.0549	.0524	.0522	
$N/(\frac{C_s}{C_f})^{.35}(Re)^{.705}(Pr)^{.72}$	.0984					6260	6260	6260	6260	6260		
$(D/D_s)^{.05}$	1.555											
$(D/D_s)^{-.152}$	.265											
$(K_s/K_f)^{.05}$	1001											
$(K_s/K_f)^{.08}$	1005											

1	2	3	4	5	6	7	8	9	10	11
1.06	1.06									1.06
2.5	2.5	2.5	2.5	2.5	2.5	2.5	2.5	2.5	2.5	2.5
.214	.214	.214	.214	.214	.214	.214	.214	.214	.214	.214
3310	3310	3310	3310	3310	3310	6580	6580	6590	6590	6580
.584	.584	.584	.584	.584	.584	.584	.584	.584	.584	.584
.968	.968	.968	.968	.968	.968	.938	.938	.938	.937	.934
1.019	1.019	1.019	1.019	1.019	1.019	1.040	1.040	1.040	1.040	1.040
2.54	2.54	2.54	2.54	2.54	2.54	5.06	5.06	5.06	5.06	5.06
269000	392000	169800	139000	240000	344000	333000	251000	257000	190500	121000
.00716	.00716	.00716	.00716	.00716	.00716	.00716	.00716	.00716	.00716	.00716
140	244	48.4	70.5	12.6	183	165	142	136	99.6	46.0
.9785	.9785	.9785	.9785	.9785	.9785	.9583	.9583	.9583	.9583	.9583
.093	.070	.172	.106	.091	.075	.088	.086	.0845	.096	.142
3800	9600	650	1250	3200	6000	5000	4000	3700	2.80	610
.377	.279	.79	.500	.431	.362	.367	.35	.398	.444	.672
90	173	37.4	54.8	88.6	137	111	97.5	99.5	74	37.4
527	917	219	320	520	800	652	574	585	429	219

TABLE NO. 10

Calculated Data - Snowflake White Slurry Run

Run No.	1	2	3	4	5	6	7	8	9	10	11	12	Run No.
Friction Factor, f	.0192	.0213	.0210	.0222	.0233	.0310	.0308	.0252	.0230	.0216	.0204	.0198	K_s/K_f
1 $\sqrt{f}$	7.21	6.85	6.90	6.71	6.55	5.68	5.70	6.92	6.60	6.80	7.00	7.11	D_s Mic.
Re $\sqrt{f}$	10500	6800	7200	5800	4800Ø	1700	1770	3550	5100	6400	8200	9200	C_s/Cf
Reynolds No., RE x 10^3	75.5	46.6	49.6	38.9	31.4	9.65	10.1	22.3	33.6	43.5	57.3	65.2	Ft^2/Ft^3
Bulk Viscosity u_b, lbs/min.ft.	.0184	.0255	.0215	.0225	.0224	.0436	.0493	.0308	.0256	.0238	.0216	.0211	$(C_s/C_f).35$
Corrected Bulk Viscosity, u'_b	.0192	.0247	.0212	.0221	.0221	.0421	.0459	.0304	.0256	.0240	.0218	.0214	C Slurry Average
Corrected Reynolds No. x10^3	72.4	48.1	50.4	40.6	31.8	9.95	10.2	22.3	33.6	43.1	56.8	64.3	P_{sl} gm/cc
Mass Fraction, solid in slurry, x	.048	.048	.048	.048	.048	.048	.104	.104	.104	.104	.104	.104	# Snowflake/Ft^3 Slurry
Temp.Drop across Pipe wall, t_m °F	11.9	11.0	10.6	9.8	9.0	7.0	7.6	9.2	10.8	11.5	12.2	12.7	h 1.67
Inside Pipe Wall Temp., t_{si}, °F	193.1	197.0	198.4	204.2	204.0	210.0	210.4	203.8	208.2	202.5	198.8	198.3	D 1.67
Log Mean Temp. Differ., t_{lm}, °F	46.1	49.0	51.1	54.3	57.3	60.1	65.0	57.2	57.4	52.7	49.8	46.6	$N/(pr)\cdot^{04}$
Slurry Heat, BTU/hr. x10^3	181	161	158	143	123	89	95.8	119	142	154	165	172	$C_{sl\ Av.}^{.667}$
Steam Heat, BTU/hr. x 10^3	179	166	159.5	147.5	133.5	105.4	114.2	139	163.3	172.9	184.7	192	u .667
Film Coefficient, BTU/hr.ft^2 °F	3020	2530	2380	2030	1650	1140	1135	1600	1900	2180	2550	284-	$(N/(pr)\cdot^{04})^{1.67}$
Nusselt Number, N	414	346	326	278	226	156	156	219	260	299	350	389	K_e
Prandtl Number, P	3.05	3.92	3.36	3.51	3.51	6.69	7.75	4.83	4.06	3.81	3.46	3.40	$N/(pr)^{.72}(\frac{Ks}{Kf})^{.05}(\frac{D}{Ds})^{.05}(\frac{Cs}{Cf})^{.3}$
$P^{.72}$	2.18	2.60	2.34	2.41	2.41	3.78	4.20	3.01	2.66	2.62	2.38	2.35	$N/(Pr)^{.72}(\frac{Ks}{Kf})^{.08}(\frac{D}{Ds})^{-.152}(\frac{Cs}{Cf})^{.3}$
$N/P^{.72}$	190	133	139	115	93.8	41.3	37.2	72.8	97.7	121.0	147.0	165.0	
$Re^{.7}$	2660	2000	2070	1770	1480	656	667	1160	1540	1860	2250	2460	
$N/P^{.72}\ Re^{.7}$	.0714	.0665	.0671	.0650	.0634	.0629	.0558	.0628	.0634	.0630	.0653	.0670	Av.0646
D/D_s	2610	2610	2610	2610	2610	2610	2610	2610	2610	2610	2610	2610	
$N/(\frac{C_s}{C_f})^{.35}(Re)^{.705}(Pr)^{.72}$	1.11												
$(D/D_s)^{.05}$	1.482												
$(D/D_s)^{-.152}$	.304												
$(K_s/K_f)^{.05}$	1.001												
$(K_s/K_f)^{.08}$	1.005												

1	2	3	4	5	6	7	8	9	10	11	12
1.06	1.06	1.06	1.06	1.06	1.06	1.06	1.06	1.06	1.06	1.06	1.06
6	6	6	6	6	6	6	6	6	6	6	6
.214	.214	.214	.214	.214	.214	.214	.214	.214	.214	.214	.214
1235	1235	1235	1235	1235	1235	2770	2770	2770	2770	2770	2770
.584	.584	.584	.584	.584	.584	.584	.584	.584	.584	.584	.584
.962	.962	.962	.962	.962	.962	.918	.918	.918	.918	.918	.918
1.026	1.026	1.026	1.026	1.026	1.026	1.058	1.058	1.058	1.058	1.058	1.058
3.07	3.07	3.07	3.07	3.07	3.07	6.85	6.85	6.85	6.85	6.85	6.85
640000	495000	427000	331000	229000	125700	125600	223900	288200	398000	501000	575000
.00716	.00716	.00716	.00716	.00716	.00716	.00716	.00716	.00716	.00716	.00716	.00716
23.3	16.5	17.3	14.5	118	46.5	47.1	89	125	152	190	222
.9745	.9745	.9745	.9745	.9745	.9745	.9445	.9445	.9445	.9445	.9445	.9445
.072	.084	.077	.078	.120	.134	.097	.097	.0865	.0825	.0775	.0765
9200	5000	5500	4100	2900	600	630	1800	3200	4400	6450	8400
.463	.563	.480	.495	.482	.834	.736	.63	.515	.541	.495	.440
218	153	1595	133	108	47.5	42.7	83.6	112	139	168	189.8
1065	245	780	648	526	232	209	408	549	680	825	928

TABLE NO. 11

Calculated Data - No. 1 White Slurry Runs

Run No.	1	2	3	4	5	6	7	8	9	10
Friction Factor, f	.0328	.0230	.0236	.0258	.0267	.0214	.0228	.0224	.0256	.0261
$1/\sqrt{f}$	6.62	6.59	6.50	6.22	6.11	6.85	6.62	6.70	6.25	6.22
Re $\sqrt{f}$	5200	5000	4500	3300	2600	6800	5200	5800	3400	3300
Reynolds Number, RE ($\times 10^3$)	34.4	32.8	29.2	20.5	15.95	46.5	34.4	38.9	21.2	20.5
Bulk Viscosity u_b, lbs/min., ft.	.0339	.0314	.0322	.0406	.0386	.0284	.0316	.0223	.0307	.0272
Corrected Bulk Viscosity, u'_b	.0322	.0296	.0311	.0384	.0357	.0271	.0344	.0214	.0294	.0262
Corrected Reynolds Number ($\times 10^3$)	36.2	34.8	31.2	21.7	17.2	48.8	31.6	40.5	22.2	21.3
Mass Fraction, solid in slurry, x	.056	.056	.056	.056	.056	.115	.115	.115	.115	.115
Temp. Drop across Pipe wall, t_m °F	11.0	10.3	9.6	9.2	8.0	12.1	10.8	9.5	8.4	7.5
Inside Pipe Wall Temp., t_{si}, °F	198	200	199	202	209	196	197	204	210	211
Log Mean Temp.Difference, t_{lm}, °F	50.8	49.6	46.3	51.6	56.7	46.1	53.5	50.5	59.5	62.9
Slurry Heat, BTU/hr ($\times 10^3$)	165	156	145	138	120	169	154	139	117	105
Steam Heat, BTU/hr ($\times 10^3$)	158	162	150	114	137	183	162	143	126	113
Film Coefficient, BTU/hr ft^2 °F	2500	2420	2410	2060	1630	2820	2210	2120	1510	1280
Nusselt Number, N	342	332	330	282	223	386	302	290	207	176
Prandtl Number, P	5.11	4.70	4.94	6.09	5.66	4.30	5.45	3.40	4.66	4.15
$P^{.72}$	3.12	2.95	3.06	3.54	3.36	2.78	3.28	2.35	2.94	2.70
$N/P^{.72}$	110.0	112.0	108.0	79.7	66.4	139.0	92.0	123.0	70.4	65.3
$Re^{.7}$	1640	1590	1470	1140	964	2020	1480	1770	1160	1120
$N/P^{.72}\ Re^{.7}$	.0671	.0705	.0734	.0700	.0688	.0688	.0621	.0694	.0606	.0583
D/D_s	1120	1120	1120	1120	1120	1120	1120	1120	1120	1120
$N/\left(\frac{C_s}{C_f}\right)^{.35}(Re)^{.705}(Pr)^{.72}$	.118									
$(D/D_s)^{.05}$	1.42									
$(D/D_s)^{-.152}$	.343									
$(K_s/K_f)^{.05}$	1.001									
$N/(Pr)^{.72}\left(\frac{K_s}{K_f}\right)^{.08}\left(\frac{D}{D_s}\right)^{-0.15}\left(\frac{C_s}{C_f}\right)^{0.35}$	546	560	536	396	330	690	457	614	350	325

Av. .0691

Run No.	1	2	3	4	5	6	7	8	9	10
K_s/K_f	1.06	1.06	1.06	1.06	1.06	1.06	1.06	1.06	1.06	1.06
D_s Mic.	14	14	14	14	14	14	14	14	14	16
C_s/C_f	.214	.214	.214	.214	.214	.214	.214	.214	.214	.214
Ft^2/Ft^3	.835	.835	.835	.835	.835	1765	1765	1765	1765	1765
$(C_s/C_f)^{.35}$	.584	.584	.584	.584	.584	.584	.584	.584	.584	.584
$C_{Slurry\ Aver.}$	.956	.956	.956	.956	.956	.909	.909	.909	.909	.909
Psl gm/cc	1.032	1.032	1.032	1.032	1.032	1.07	1.07	1.07	1.07	1.07
#1 White/Ft^3 Slurry	3.61	3.61	3.61	3.61	3.61	7.66	7.66	7.66	7.66	7.66
$(K_s/K_f)^{.08}$	1.005	1.005	1.005	1.005	1.005	1.005	1.005	1.005	1.005	1.005
$h^{1.67}$	457000	447000	447000	338000	229000	575000	392000	363000	199000	156000
$D^{1.67}$	.00716	.00716	.00716	.00716	.00716	.00716	.00716	.00716	.00716	.00716
$N/(Pr)^{.04}$	130	127	118	88	72	168	117	145	89	86
C average $^{.667}$	.9705	.9705	.9705	.9705	.9705	.9355	.9355	.9355	.9355	.9355
$u^{.667}$	103	.0985	.1025	.117	.113	.0924	.0986	.0786	.0975	.0895
$(N/(Pr)^{.04})^{1.67}$	3400	3250	2900	1780	1290	5200	2850	4100	1800	1700
K_e	.625	.671	.721	.770	.752	.595	.693	.558	.568	.512
$N_n/(Pr)^{.72}\left(\frac{K_s}{K_f}\right)^{.05}\left(\frac{D}{D_s}\right)^{.05}\left(\frac{C_s}{C_f}\right)^{.35}$	131.5	135	129.0	95.5	80.5	1669	110	147.3	84.3	78

TABLE NO. 12

Calculated Data - Copper Slurry Runs

Run No.	1	2	3	4	5	6	7
Friction Factor, f	.0205	.0234	.0214	.0231	.0254	.0251	.0296
$1/\sqrt{f}$	6.98	6.53	6.83	6.60	6.28	6.32	5.82
Re $\sqrt{f}$	8000	4950	6700	5100	3555	3700	2040
Reynolds No., RE	55800	32400	46800	33700	22300	23600	11900
Bulk Viscosity u_b, lbs/min. ft.	.0233	.0339	.0206	.0214	.0354	.0266	.0401
Corrected Bulk Viscosity, u'_b	.0240	.0351	.0214	.0211	.0355	.0253	.0378
Corrected Reynolds No. x 10^3	54	31.3	45.1	34.2	22.2	24.8	12.6
Mass Fraction, solid in slurry, x	.030	.030	.030	.030	.030	.030	.030
Temp.Drop across Pipe Wall, t_m °F	12.25	11.60	11.21	9.4	9.9	8.55	7.5
Inside Pipe Wall Temp., t_{si}, °F	195.7	203.4	203.3	202.1	202.4	209.2	212.8
Log Mean Temp. Difference, t_{lm}, °F	48.2	51.3	53.3	53.6	51.0	59.0	65.0
Slurry Heat, BTU/hr. x10^3	184.5	175	169	142	149.2	129	103
Steam Heat, BTU/hr. x10^3	188	192	1755	146	155.5	132	118.4
Film Coefficient, BTU/hr. ft.^{2} °F	2940	2630	2440	2040	2250	1680	1400
Nusselt Number, $N = \frac{hD}{K}$	403	359	334	279	308	230	192
Prandtl Number, $P = \frac{Cu}{K}$	3.81	5.56	3.38	3.35	5.63	4.02	6.00
$P^{.72}$	2.55	3.33	2.35	2.33	3.35	2.65	3.51
$N/P^{.72}$	158	109	142	120	92	87	54.7
$Re^{.7}$	2150	1443	1858	1548	1125	1224	763
$N/P^{.72}Re^{.7}$	.0735	.0754	.0764	.0776	.0816	.0771	.0711 (Av. .0762)
D/D_s	520	520	520	520	520	520	520
(*)	.174	.174	.174	.174	.174	.174	.174
$(D/Ds)^{.05}$	1.368	1.368	1.368	1.368	1.36	1.368	1.368
$(D/Ds)^{-.152}$	.386	.386	.386	.386	.386	.386	.386
$(K_s/K_f)^{.05}$	1.374	1.374	1.374	1.374	1.374	1.374	1.374
(**)	646	384	506	426	327	309	195

Run No.	1	2	3	4	5	6	7
K_s/K_f	582	582	582	582	582	582	582
D_s Mic.	30.16	30.16	30.16	30.16	30.16	30.16	30.16
C_sC_f	.0932	.0932	.0932	.0932	.0932	.0932	.0932
Ft^2/Ft^3	205	205	205	205	205	205	205
(C_s/C_f) .35	.437	.437	.437	.437	.437	.437	.437
C slurry Average	.973	.973	.973	.973	.973	.973	.973
P gm/cc	1.015	1.015	1.015	1.015	1.015	1.015	1.015
#Copper/Ft^3 Slurry	1.90	1.90	1.90	1.90	1.90	1.90	1.90
(K_s/K_f) .08	1.665	1.665	1.665	1.665	1.665	1.665	1.665
h 1.67	630000	512000	447000	331000	398000	390000	178000
D 1.67	.00176	.00176	.00176	.00176	.00176	.00176	.00176
$\frac{hD}{K}/(\frac{Cu}{K})$.04	183	118	159	126	89	98	56
C average.667	.9819	.9819	.9819	.9819	.9819	.9819	.9819
u .667	.0825	.107	.0765	.076	.1075	.0855	.112
$(\frac{hD}{K})/(\frac{Cu}{K})^{.04}$	6000	2900	4700	3200	1800	2150	840
K_e	.603	.784	.57	.645	.975	1.01	.898
V_c Ft/Sec	6.61	5.60	4.92	3.68	4.02	3.20	2.42
$N_n/(Pr)^{.72}(\frac{ks}{kf})^{.05}(\frac{D}{Ds})^{.05}(\frac{Cs}{Cf})^{.35}$	221.0	158.1	190.5	145.2	111.5	105.2	66.4

(*) $N/(\frac{C_s}{C_f})^{0.35}(Re)^{.705}(Pr)^{.72}$

(**) $N/(Pr)^{.72}(\frac{K_s}{K_f})^{.08}(\frac{D}{D_s})^{-0.15}(\frac{C_s}{C_f})^{0.35}$

TABLE NO. 13
Observed and Calculated Data
From Salamone (15) for Figures 7 and 12

Film Coeffic. h	Nusselt Number N	Prandtl Number P	N .72 P	Reynolds Number RE	Ordinate of Figure	Run No.
3575	490	3.46	201	143,800	223.0	89
3072	421	3.59	168	119,600	187.0	90
3076	422	3.72	164	109,200	183.0	91
2644	363	4.04	133	83,300	147.8	92
2373	325	4.35	113	66,500	125.5	93
3531	483	4.30	190	117,000	189.0	94
3256	445	4.35	154	105,500	154.5	95
2974	408	4.55	137	87,200	152.8	96
2563	352	4.74	115	70,600	128.0	97
2190	300	5.13	93	53,600	103.2	98
3491	478	4.89	153	105,300	171.0	99
3141	431	5.61	125	92,800	151.0	100
2978	408	5.06	127	82,500	141.5	101
2684	368	5.25	112	69,200	124.5	102
2289	314	5.64	90	53,100	101.0	103
1703	234	6.58	60	31,100	67.0	104

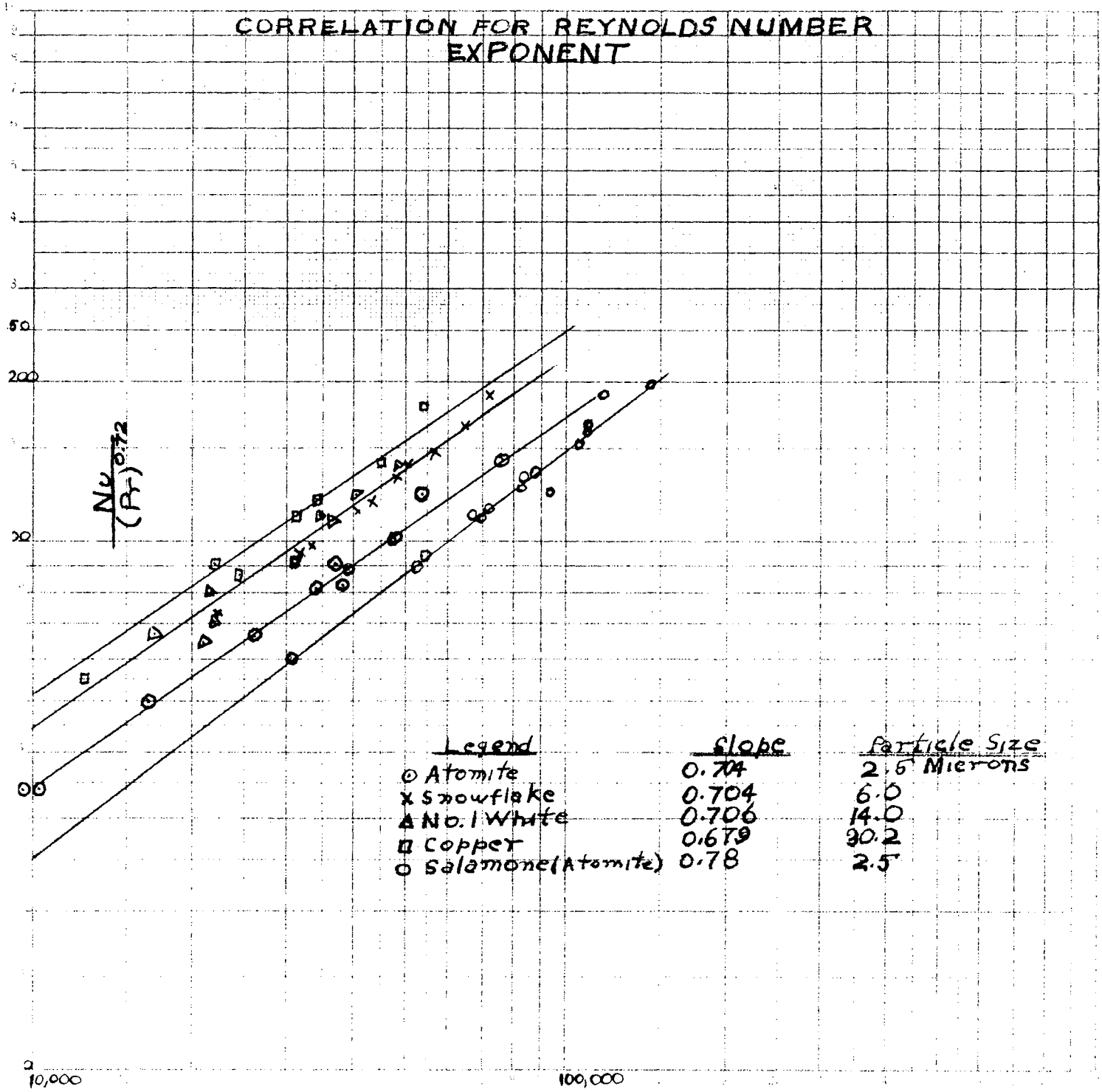
CORRELATION FOR REYNOLDS NUMBER EXPONENT
$\frac{Nu}{(Pr)^{0.72}}$
50
200
10,000
100,000
Re'
Legend
Atomite
Snowflake
No. 1 White
Copper
Salamone (Atomite)
Slope
0.704
0.704
0.706
0.679
0.78
Particle Size
2.6 Microns
6.0
14.0
30.2
2.5

Fig. 7

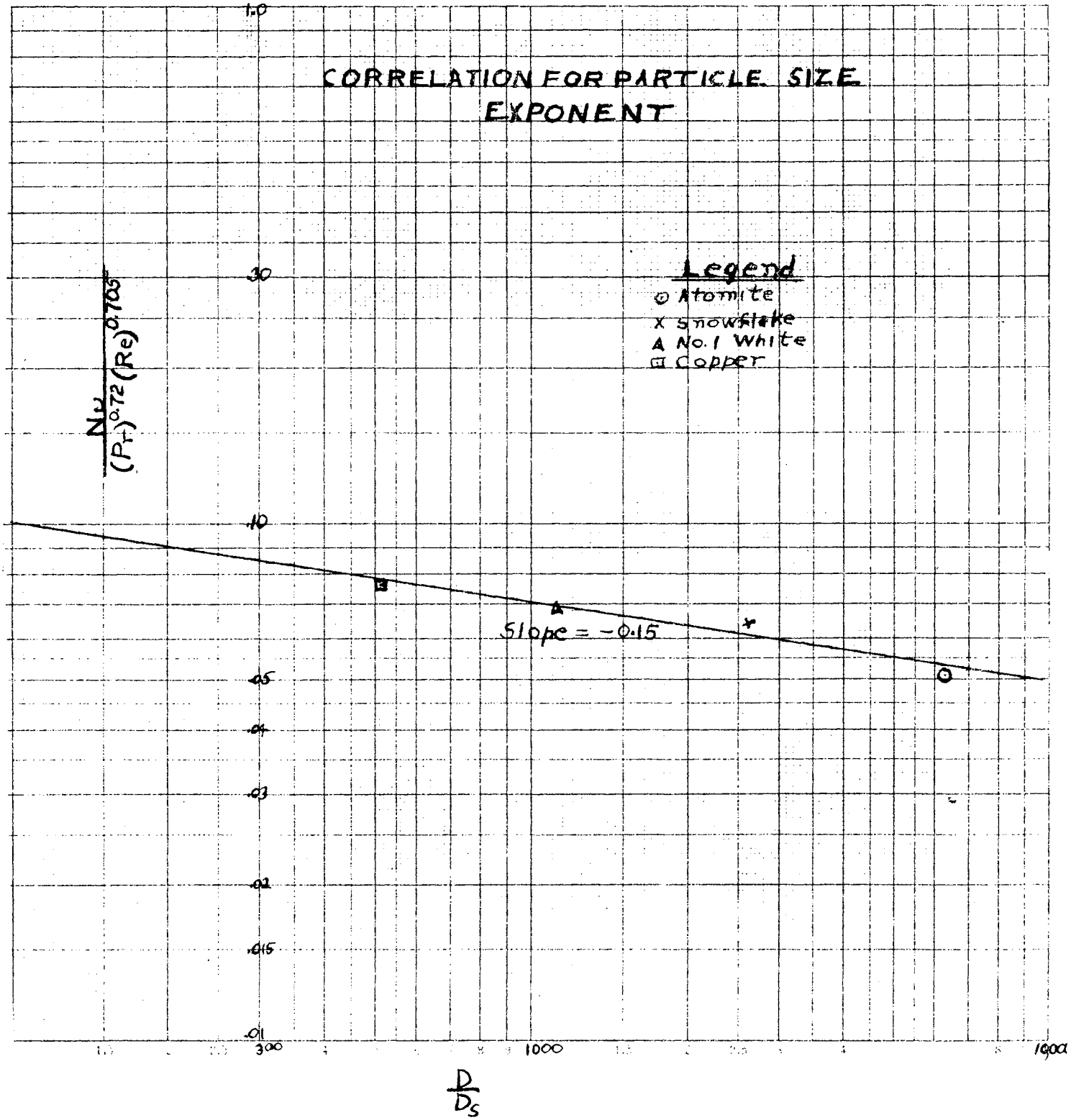
CORRELATION FOR PARTICLE SIZE EXPONENT
Legend
Atomite
Snowflake
No. 1 White
Copper
Slope = -0.15
$\frac{Nu}{(P_r)^{0.72}(Re)^{0.705}}$
1.0
.30
.10
.05
.04
.03
.02
.015
.01
300
1000
1900
$\frac{D}{D_s}$

Fig. 8

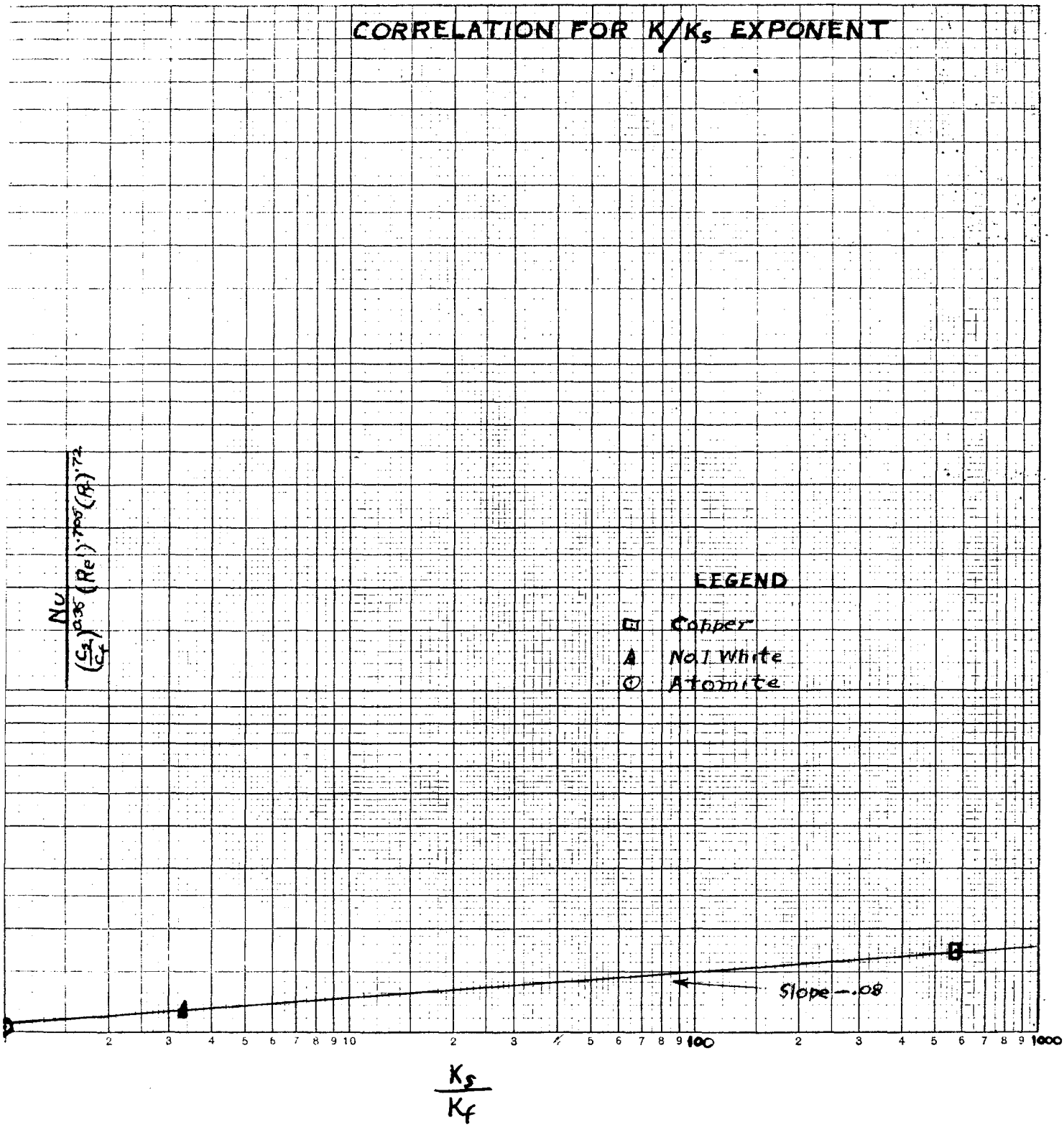
CORRELATION FOR K/Ks EXPONENT
LEGEND
Copper
No.1 White
Atomite
Slope -.08
$\frac{Nu}{(\frac{C_s}{C_f})^{.035}(Re)^{.705}(A)^{.72}}$
$\frac{K_s}{K_f}$

Fig. 9

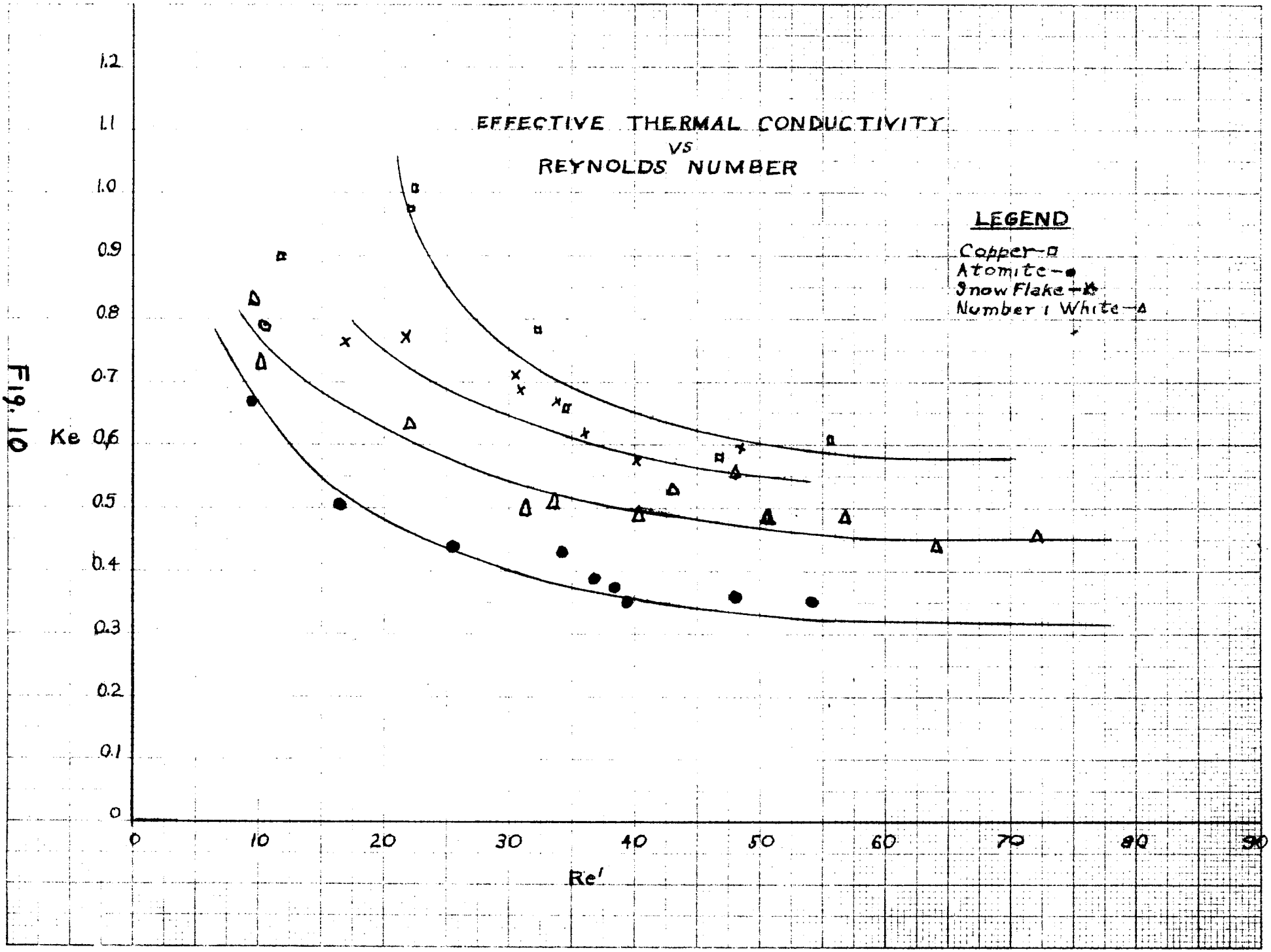
EFFECTIVE THERMAL CONDUCTIVITY
VS
REYNOLDS NUMBER
LEGEND
Copper-□
Atomite-●
Snow Flake-✱
Number 1 White-△
Ke
Re'
1.2
1.1
1.0
0.9
0.8
0.7
0.6
0.5
0.4
0.3
0.2
0.1
0
0
10
20
30
40
50
60
70
80
90

Fig. 10

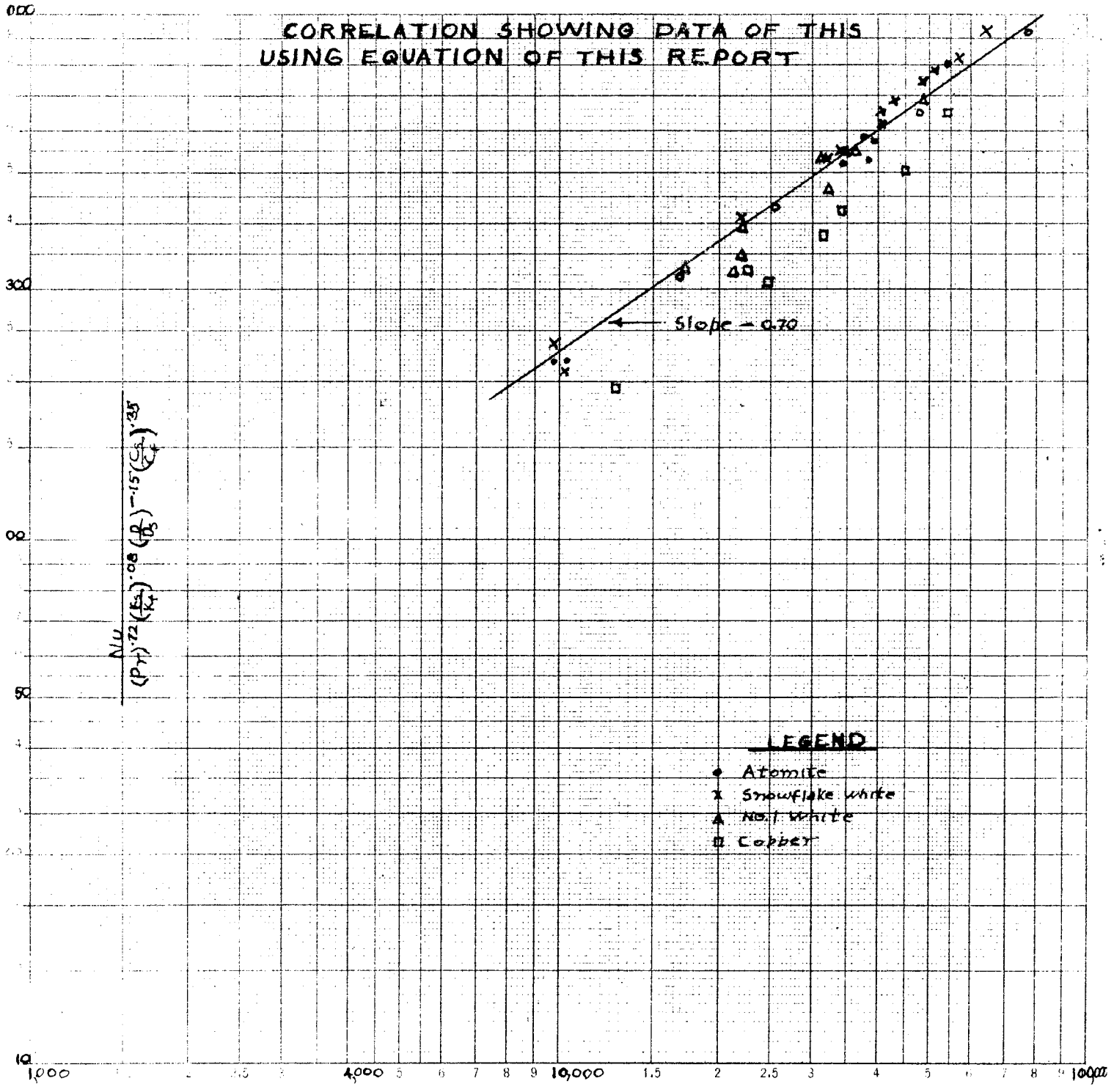
CORRELATION SHOWING DATA OF THIS
USING EQUATION OF THIS REPORT
Slope = 0.70
LEGEND
Atomite
Snowflake white
No.1 White
Copper
Re' corrected

Fig. 11

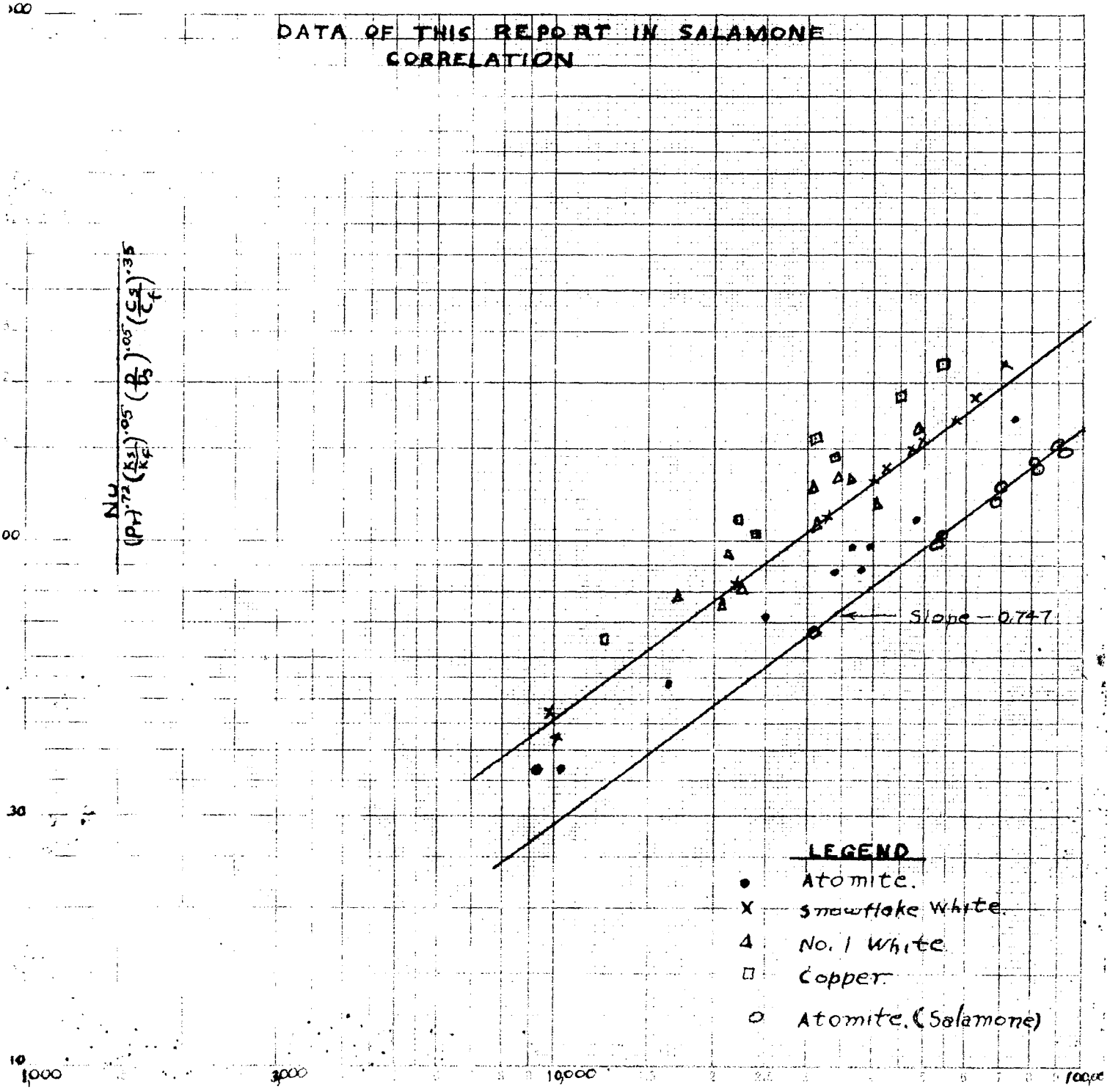
DATA OF THIS REPORT IN SALAMONE CORRELATION
$\frac{Nu}{(Pr)^{.72}(\frac{k_s}{k_f})^{.05}(\frac{\rho_s}{\rho_f})^{.05}(\frac{c_s}{c_f})^{.35}}$
Slope = 0.747
LEGEND
Atomite.
Snowflake White.
No. 1 White
Copper.
Atomite. (Salamone)
1000
3000
10,000
Re' Corrected

Fig. 12

DISCUSSION OF RESULTS

The results of this investigation tend to show that the coefficient of heat transfer to non-Newtonian suspensions depends mainly on three groups in equation 12; the Nusselt, Reynolds, and Prandtl, whose appearance would be expected because in most cases of heat transfer in forced convection the relation takes the form of the Nusselt group as a function of the other two; and that the components of the Reynolds and Prandtl groups should be based on the properties of the slurry involved.

The C_s/C_f group (ratio of specific heats) is the only other group of any significance, its exponent being 0.35. This indicates that the convective transport of heat due to the particles in suspension is important in the mechanism of heat transfer.

It was further substantiated that the effective thermal conductivity of the suspensions increased with decreasing flow rates and that K_e approaches some limiting value which appears higher than that for the thermal conductivity of water at Reynolds numbers in the fully turbulent region as is shown by the flattening of the curves in Figure 10 in the higher Reynolds number regions. This family of curves also indicates that increased particle size tends to raise the effective thermal conductivities.

Figure 10 further indicates that the K_e of the slurry may have been increased above that of the dispersion

medium alone by two mechanisms: (1) an increased turbulence produced by the solid particles, and (2) an increase in heat transfer due to interparticle conduction and to conduction between particles and pipe wall.

The first effect will be produced by any kind of particles. The second effect will be more pronounced when particles whose thermal conductive is very high compared to the dispersion medium used.

From a previous statement referring to Figure 10, it seems that the K_e should increase with increasing slurry rates due to an increase in turbulence, this is only true for most cases where the conductivities of water, the suspension medium, and slurries are compared. This is not a characteristic of the slurry. The decrease of K_e of the slurries with greater flow rates can be attributed to an increase in turbulence, although this increase reduces the film thickness and allows more contacts per unit time between particles and pipe wall and particles, it reduces the wall particle contact time (which is the greatest driving force of the heat transfer mechanism) to a degree where very little heat is conducted from wall to particle. This reduces the amount of heat the rest of the slurry can receive by conduction to other particles and the dispersion medium. The

mechanism reverses as the rate of flow decreases.

Salamone(15)states that where the liquid and solid conductivity is nearly the same the effective thermal conductivity is practically independent of flow rate. This may be true for most of the turbulent region. However, Figure 10 shows that in the lower extremities of the turbulent flow region that there is a definite tendency for the effective thermal conductivity to increase. In addition, Figure 10 shows this effect is more apparent for copper which has a much higher thermal conductivity than chalk.

The original formula did not contain a (K_s/K_f) term but by re-arranging terms this group was found and its exponent was 0.05. This exponent was checked by plotting the log of K_s/K_f against the log of the equation, Figure 9. The calculated slope of the curve which is the exponent of the term was found to be 0.08 which checks the original equation accuracy. This low exponent indicates that the thermal conductivity of the particle effects the coefficient of heat transfer very little unless the K_s/K_f is very large in magnitude. This is perhaps due to the fact that the mass of solid to the mass of the dispersion medium is a very small ratio. In order for the conductivity of the solid to have an effect on the film coefficient, its conductivity must be very large as

is shown by the slight increase between the point for chalk and that of copper.

However, from Figure 10, in the lower turbulent regions K_e increases rapidly as a function of increasing thermal conductivity and/or particle size of the suspended solid. Therefore, in this region it would be expected that the thermal conductivities of the solid would have more effect on the magnitude of the film coefficient and that the effective thermal conductivity must be calculated at the specific Reynolds number for use in the Dittus-Boelter equation, $N_u = (Re)^{0.8} (Pr)^{0.4}$

The D/D_s term whose exponent was determined from Figure 8 tends to show that the film coefficient increases with increasing particle size. This is substantiated by Figure 10 which indicates the larger the particle size the larger the effective thermal conductivity.

From the previous discussion, it appears that the physical properties of the particle is a critical factor in the determination of the film coefficient and those taken into account were the thermal conductivity and the average mesh size diameter. The assumption, that the particle shape was a sphere is not necessarily true, and the true particle shapes if determined and used would alter curves and exponents to various degrees, and it would seem that the greatest change would be seen in the

D/D_s value of Equation 12.

A plot of the new equation and J. J. Salamone equation Figure 12 shows the lines to be offset but parallel. Perhaps this could be explained in that Salamone's line is based on mostly copper slurry runs and the new line, Equation 12, being based on mostly chalk runs; however, the greatest contributing factor toward this displacement is probably due to the method in which the thermocouples were attached to the 1/2 inch pipe. In Salamone (15) the thermocouple leads which were wrapped around the 1/2 inch pipe.were subject to heat flow through the wire from the steam jacket to the junction which would give a higher temperature reading, thus introducing an appreciable error. This error in the Δt_{lm} which appears in the denominator of the expression for the film coefficient, h, would give lower values than the values calculated in this report, inasmuch as the thermocouple leads in this apparatus were sealed into linear grooves along the outside surface of the heat transfer area and therefore not subject to the error of a higher temperature reading at the pipe wall.

The investigators felt that if results of all the copper runs which were made could have been utilized the spread between the original equation and the new equation 12 would have been reduced. This could not be done because a large number of the copper runs had to be discarded due to a faulty pump and additional runs could

not be made because all the available pumps were found to be in the same condition or inappropriate for these abrasive slurries.

The final correlations represented by equations 12 and 3 cannot be taken to indicate completely the mechanism of heat transmission because they are only an empirical representation of the results which are in accord with the concepts of dimensional analysis.

SUMMARY and CONCLUSIONS

Water suspensions such as those used in this investigation (solid powders of copper and chalk) behave as pseudo-plastic non-Newtonian solutions whose apparent viscosity decreases with increasing rates of flow. In flow ranges of maximum turbulence the apparent viscosity approaches a limiting value which is greater than the viscosity of the dispersion medium. Due to their non-Newtonian characteristics, standard design equations for Newtonian liquids cannot be used for heat transfer calculations for non-Newtonian suspensions.

The original equation (1) and the equation (12) correlated from this investigation substantially agree as can be seen in Figure 9 which utilizes the experimental data from this investigation in both equations.

The above mentioned equations may be utilized for design equations for heat transfer to solid liquid suspensions in turbulent flow inside pipes, provided that the apparent viscosities used are at the existing flow conditions of the suspensions. For suspensions whose particles are of high thermal conductivities, the original Equation 3 of J. J. Salamone is recommended and for suspensions whose particles have a low thermal conductivity Equation 12 of this investigation may give better results.

In the final analysis of the data, several questions presented themselves in which the investigators felt that the particle diameter should have been calculated from a sphere having the same volume as the particle in question. For example, the average mesh size for copper, whose crystals are face centered cubes, should have been multiplied by a factor of 1.24, Brown (7). This would undoubtedly change the exponent of the $\frac{D}{D_s}$ group and would change the slope of the lines in Salamone's (15) (Plot 22) which are for determining effective thermal conductivities at Reynolds numbers over 50,000 based on a weight of solid in suspension.

The investigators feel that not enough is known as to the effect, if any, that the actual particle shape has on the heat transfer mechanism. We assume from the collected data that copper gives a higher effective thermal conductivity than chalk due to its larger particle size and higher thermal conductivity. However, an investigation should be made using materials of approximately the same thermal conductivity, particle size, and weight fraction based on the density of the solid (to insure a nearly equal number of particles) but having different crystaline shapes. Under these equal conditions and assuming equal contact time, it could be shown whether the shape has any effect on the heat transfer mechanism.

The tendency for the larger particle slurries to have larger effective thermal conductivity presents another problem as to how large a particle can be utilized.

The investigators feel that when the above and possible other points not brought out here are looked into, a much broader and clearer concept of the heat transfer mechanisms involved will be realized.

NOTATIONS and UNITS

a - Constant, no dimensions

A - Heat transfer surface - Sq. Ft.

b - Constant, no dimensions

C_f - Specific heat of fluid or suspending medium BTU/(lb_m) (degree F)

C_b - Average specific heat of slurry solution BTU/(lbm)(degree F)

C_s - Specific heat of suspended solid BTU/(lbm)(degree F)

D - Pipe diameter, Ft.

D_s - Average diameter of suspended solid particles, ft.

e - Constant, no dimensions

f - Friction factor, dimensionless; constant, no dimensions; fluid

g - Constant, no dimensions

g_c - Dimensional constant, 32.2 (lbm)(ft)/(lb_f)(sec)^2

h - Film coefficient of heat transfer BTU/(hr)(sq.ft)(degree F)

i - Constant, no dimensions

j - Constant, no dimensions

Kl,K- Thermal conductivity of fluid or suspending medium BTU/(hr)(degree F)

K_b - Bulk thermal conductivity of suspension BTU/(hr) (degree F)(ft.)

K_e - Effective thermal conductivity of suspension BTU/(hr)(degree F)(ft.)

K_s - Thermal conductivity of suspended solid BTU/(hr)(degree F)(ft.)

K'_e- Average effective conductivity of slurry at Reynolds number 50,000 BTU/(hr)(degree F)(ft.)

L - Length of pipe, (ft); any linear dimension

m - Any mass dimension; mean

n - Constant, no dimension

Θ - Time dimension

P_f - Density of fluid, lb_m/ cu. ft. - P_f

P_s - Density of solid, lb_m/cu. ft.

P_b - Bulk density of slurry, lb_m/cu. ft.

ΔP - Pressure drop over length of pipe, L, (lb_f)/sq. ft.

q - Heat transfer rate, BTU/hr

r - Constant, no dimension

t - Temperature, degree F, any temperature dimension

tm-Temperature drop across pipe wall, degree F.

t_{s1}- Temperature of inside pipe surface, degree F.

Δt_{lm}-Logorithmic mean temperature difference between average inside pipe surface temperature and inlet and outlet slurry temperature, degree F.

V - Linear velocity, ft/sec.

V_b - Linear velocity of slurry, based on bulk density of the slurry, ft/sec.

$u_1 u_f$- Viscosity of fluid, lbs/ft.-sec.

u_w - Viscosity of fluid at wall temperature

u_b - Apparent bulk viscosity of slurry

X_1 - Weight fraction of solid

X_w - Pipe wall thickness, inches

Z - Constant, no dimensions

BIBLIOGRAPHY

1. Alves, G. E., Chemical Engineering, Vol. 56, May, 1949 p. 107

2. American Institute of Physics, "Temperature, Its Measurement and Control in Science and Industry," Rheinhold Publ. Corp., New York, 1941, p. 855-61.

3. Babbit, H. E., and Caldwell, D. H., Industrial Engineering Chemistry, Vol. 33, 1941, p. 249.

4. Binder, R. C. and Busher, J. E., (Tr.A.S.M.E.) Journal of Applied Mechanics, Vol. 23, 1946, A. 101.

5. Bingham, E. C., "Fluidity & Plasticity," Mc-Graw-Hill Book Co., Inc., New York, 1922.

6. Bonilla, C. F., et al. "Preprints of Symposium on Heat Transfer," 44th Annual Meeting A.I. ChE., Dec., 1951

7. Brown, G. G. and Associates, "Unit Operations" New York, John Wiley and Sons, Inc., 1950, Ch. 12.

8. Chu, J. C., Brown, F., and Burridge, K. C., Industrial Engineering Chemistry, Vol. 45, 1953, p. 1685

9. MacLaren, D. D. and Stairs, R. G., Master's Thesis in Chemical Engineering, Columbia University, 1948.

10. McAdams, W. H., "Heat Transmission," New York, Mc-Graw-Hill Book Co., 1942.

11. Hoopes, J. W., et al., Ch. E. S-111 Report, Columbia University, 1945.

12. Munroe, W. D. & Amundson, N. R., Industrial and Engineering Chemistry, Vol. 42, August 1950, p. 1481-88.

13. Orr, C., Jr., and Dalla Valle, J. M., Preprint No. 13, Heat Transfer, 44th Annual Meeting A.K. Ch.E.,Dec.,1953.

14. Perry, J. H. (Editor), "Chemical Engineers Handbook," New York, McGraw-Hill Book Co., Inc., 1950.

15. Salamone, J. M., Doctor of Engineering Science Thesis, New York University, April 1954.

16. Shandling, J., Master's Thesis in Chemical Engineering, New York University, 1949.

17. Wilhelm, R. H. and Wroughton, D. M., Industrial Engineering Chemistry, Vol. 31, 1939, p. 482.

18. Wilhelm, R. H., Wroughton, D. M., and Lieffel, W. F., Industrial Engineering Chemistry, Vol. 31, 1939, p.622.

19. Winding, C. C., Baumann, G. P. and Kranich, Chemical Progress, Vol. 43, 1947, p. 527, 613.

20. Sieder, E. W. and Tate, G.E., Industrial Engineering Chemistry, 28, 1429, 1936.

APPENDIX

Sample Calculations

Sample Run - Run No. 10 "Snowflake Suspension" (Refer to Tables 6 and 10.)

1. Slurry Density (p). Weight of water at 60° F required to fill 4 liter volumetric flasks is 9.688 lbs.

   Weight of slurry required to fill 4 liter flask is 10.30 lbs.

   Slurry density =

   $$62.4 \text{ lbs./ft}^3 \times \frac{10.30 \text{ lbs.}}{9.688 \text{ lbs.}} = 66.3 \text{ lbs/ft}^3$$

2. Weight % Solid = $\frac{66.3}{62.4} = 1.0629/\text{cc.}$

3. Mean Specific Heat (C) = $C_f (1 - x) + C_s x$

   C_f = Heat Capacity of Water BTU/lb °F

   C_s = Heat Capacity of Solid BTU/lb °F

   X = Weight fraction of solid

   $C = 1 (1-.104) + .209 (.104) = .918$ BTU/lb °F

4. Flow Rate (w) = 77.5 lbs./1.83 min. = 42.4 lbs/min.

5. Slurry Heat (q) = (w)(c)(Temp. Rise)

   $$= (42.4)(.918)(79.9^\circ\text{C} - 43.3^\circ\text{C})(1.8^\circ\text{F}/^\circ\text{C})$$
   $$60 \text{ mins./hr.}$$
   $$= 154{,}000 \text{ BTU/hr.}$$

6. Steam Heat (q') - From steam tables a plot of vapor enthalpy minus liquid entholpy versus steam pressure was made and from this the latent heat was taken.

   (q') = (Condensate Rate lbs/hr.) (Latent Heat BTU/lbs.)

   = (3.03 lbs./min.) (60 min./hr.) (952 BTU/lbs.)

   = 173,000 BTU/hr.

7. Viscometer Friction Factor (f)

$$f = \frac{(\Delta P)(D)\ (2g_c)}{P_b\ L\ V_b^{\ 2}}$$

D = 0.0518 ft. - ID of 1/2" Pipe

L = 6.0 ft. - Distance between Manometer Taps

$$V_b = \frac{W \text{ lbs/Min.}}{60 \text{ Sec./min} \times 66.3 \text{ lbs./ft}^3 \times .00211 \text{ ft.}^2} = 0.119\ W \text{ ft/Sec}$$

$$P = \frac{21.0 \text{ in.}}{12 \text{ in/ft.}} \times 62.4 \text{ lbs./ft}^3\ (1.6 - 1.0) = 65.5 \text{ lbs//ft}^2$$

$$f = \frac{(65.5)(.0518)\ (2)\ (32.2)}{(66.3)(6.0)(0.119 \times 42.4)^2} = 0.0216$$

8. Apparent Viscosity (u_b)

$$1/\sqrt{f} = 1/\sqrt{0.0216} = 6.80$$

From Fig. No.6 Re $\sqrt{f}$ = 6400

Reynolds Number (Re) = 6400/$\sqrt{0.0216}$ = 43,500

u_b (in viscometer) = $\frac{DG}{Re}$

$$G = \frac{W}{S} = \frac{W}{.00211 \text{ ft.}^2}$$

$$u_b = \frac{(.0518 \text{ ft})(W \text{ lbs./min})}{(.00211 \text{ ft}^2)(Re)} = 24.5\ \frac{42.4}{43,500} = .0238 \text{ lbs/min.ft}$$

Average Temperature in Heat Section = 61.6° C
Viscometer Temperature = 62.0 °C
Viscosity of Water at 61.6°C = 0.458 cps
Viscosity of Water at 62.0°C = 0.455 cps

u'_b (Corrected to Heat Sec. Temp. = $u_b\ \frac{.458}{.455}$ = 0.0240 lbs./min

9. Heat Section Reynolds number.

$$Re' = Re \times \frac{.0238}{.0240} = 43,500\ \frac{.0238}{.0240} = 43,100$$

10. Experimental Film Coefficient of Heat Transfer (h)

$h = q/A\ \Delta t_{lm}$

q = 154,000 BTU/hr (See Calculation No. 5)

A = π x 0.0518 ft. x 8.0 ft = 1.3 ft^2 (inside heated area)

Calculation of ΔT_{lm}

Average temperature from millivolt readings = 214°F
Temperature drop across pipe wall, tm

$$tm = \frac{(q)(\text{Pipe Thickness})}{(K\ \text{Metal})(\text{Aver. Area})} =$$

$$\frac{(154{,}000\ \text{BTU/hr.})(0.109/12\ \text{ft.})}{(90\ \text{BTU/hr. }^{\circ}\text{F ft.})(\text{Aver. Area})}$$

$$\text{Average area} = \pi D_{lm} L = (3.14)\left(\frac{0.840 - 0.622}{2.3 \log 0.840/.622\ \text{in}}\right)$$

$$(1\ \text{ft./12 in.} \times 8\ \text{ft.}) = 1.52\ \text{ft.}^2$$

$$tm = \frac{(154{,}000)(.109/12)}{(90)(1.52)} = 10.2^{\circ}\text{F}$$

Average Inner Surface Temp. = 214 -10.2 = 204°F

$$\Delta T_{lm} = \frac{(204 - 110) - (204-176)}{2.3 \log 204 - 110/204 - 176} = 54.4\ ^{\circ}\text{F}$$

$$h = \frac{154{,}000\ \text{BTU/hr}}{1.3\ \text{ft}^2\ (54.4\ ^{\circ}\text{F})} = 2180\ \text{BTU/hr ft}^2\ ^{\circ}\text{F}$$

11. Nusselt Number (N) = hD/K_f

K_f = 0.378 BTU-ft/hr ft^2 °F

$$N = \frac{2180 \times .0518}{.378} = 299$$

12. Prandtl Number (P_n) = $\frac{C_f u'}{K_f}$

$$P_n = \frac{(1.0\ \text{BTU/lb }^{\circ}\text{F})(0.0240\ \text{lb/min ft})(60\ \text{min/hr.})}{.0378\ \text{BTU/ft hr ft 2 0 F}}$$

Pn = 3.81

13. $P_n^{0.72} = (3.81)^{0.72} = 2.55$

14. $\frac{N_n}{P_n^{0.72}} = \frac{299}{255} = 117$

15. $$\frac{N_n}{(P_n^{0.72})(Re_n)^{0.7}} = \frac{117}{(43,100)^{.7}} = .630$$

16. $$\frac{\text{Diameter of Pipe}}{\text{Diameter of particle (assuming a sphere)}} = \frac{D}{D_s}$$

$$\frac{D}{D_s} = \frac{0.622 \text{ in.}}{.0000397 \text{ in/micron} \times 6 \text{ micron}} = 2.61 \times 10^3$$

17. Effective Thermal Conductivity

For Re = 43,100 -- ordinate of Fig. 5 = 152

$$152 = (hD/K_e)/CC_b u_b/K_e)^{.04}$$

$$K_e = \left(\frac{1}{152}\right)^{1.667} \left[\frac{(2180)(0.622/12)}{(0.9180(0.0214)(60)^{.04}}\right]$$

$$K_e = 0.541 \text{ BTU/(hr)(ft)(°F)}$$

18. Ordinate of Figure 11

$$\text{Ordinate} = \frac{\frac{hD}{k_f}}{\left(\frac{C_f u_b}{K_f}\right)^{0.72} \left(\frac{K_s}{K_f}\right)^{0.08} \left(\frac{D}{D_s}\right)^{-0.152} \left(\frac{C_s}{C_f}\right)^{0.35}}$$

$$\text{Ordinate} = \frac{308}{(3.81)^{.72} (1.06)^{.08} (.214)^{.35} (2610)^{-0.52}}$$

Ordinate = 650

19. Calculated film coefficient from Equation 12

$$\frac{hD}{K} = 0.346 (Re)^{.704} \left(\frac{K_s}{K_f}\right)^{.08} \left(\frac{C_s}{C_f}\right)^{.35} \left(\frac{D}{D_s}\right)^{-.152} (Pr)^{.72}$$

$$\frac{h \ 0.622/12}{0.378} = (0.346)(43,100)^{.704}(1.06)^{.08}(.214)^{.35} (2610)^{-.152}(3.81)^{.72}$$

$$h = 2.157 \text{ BTU/hr } ^\circ\text{F ft.}^2$$